Construction and Building Materials 304 (2021) 124608

Contents lists available at ScienceDirect

Construction and Building Materials

journal homepage: www.elsevier.com/locate/conbuildmat

Ultra-High performance concrete (UHPC) with polypropylene (Pp) and steel Fibres: Investigation on the high temperature behaviour

Francesca Sciarretta [a], Stefano Fava [b], Marco Francini [b], Luca Ponticelli [c], Mauro Caciolai [c], Bruno Briseghella [d], Camillo Nuti [e,*]

[a] Dipartimento di Culture del Progetto, Universita' IUAV di Venezia, Venice, Italy
[b] Buzzi Unicem S. p. A., via Luigi Buzzi, 6 - 15033 Casale Monferrato (AL), Italy
[c] Corpo Nazionale dei Vigili del Fuoco, Rome, Italy
[d] College of Civil Engineering, Fuzhou University, Fujian, China
[e] Department of Architecture, University Roma Tre, Rome, Italy

ARTICLE INFO

Keywords:
Ultra-High-Performance Concrete
Polypropylene fibres
Fire behaviour
Experimental tests
Spalling

ABSTRACT

Ultra-high performance concretes (UHPC) are advanced cement-based materials characterised by superior mechanical properties with respect to normal and high-strength concretes; however, their dense and compact matrix can facilitate the onset of spalling at high temperatures. This problem is often coped up by adding polypropylene (PP) fibres to the mix design, alone or with other types of fibres; steel fibres enhance the material's tensile capacity. The paper presents a series of tests on two UHPC types (150 and 180 N/mm2) with PP fibres (0.27% of volume) and variable content of steel fibres (0% to 1.92%), aimed at investigating the residual mechanical properties of the material after high temperature exposure. The experimental results are compared to available research on small UHPC specimens exposed to high temperatures, with dosages in PP fibres from 0.03% to 2%, and in steel fibres from 0 to 3%. The results of this research demonstrate that UHPCs need hybrid fibre reinforcement (PP + steel) to withstand high temperatures, and that the residual strength increases after 200 °C exposure, at all steel fibre dosages; this is in line with literature. Available research also shows that strength loss is possible in hot conditions, as found in the present research, while PP fibres alone do not always prevent the occurrence of spalling in small UHPC samples.

1. Introduction

In the last 25 years, ultra-high-performance concrete (UHPC) has been gaining attention in the field of construction industry and research, due to its very high mechanical strength, high energy absorption capacity in tension and durability [1,2]. To define this class of advanced cement-based materials, the minimum strength of 120 N/mm^2, i. e. the upper limit of high-strength concrete (HSC), is generally accepted [3]. The superior properties of UHPC are due to its peculiar mix design, which includes only fine aggregate (maximum grain diameter < 1 mm), and low water to cement ratio (generally not higher than 0,25). According to the study by Stengel and Schiessl [4], the mean quantities of the different components in UHPC mixes are outlined in Table 1, where the volume fraction is the ratio of quantity to density.

As far as structural applications are concerned, UHPCs are frequently used for joints between precast bridge decks, shear connector pockets, and retrofitting of damaged elements [5–7]. Other prominent applications are high-rise building columns, precast bridge girders and footbridges [8–11].

There is a need of experimental research on UHPC mechanical properties under fire exposure (or 'hot' properties), as well as after heating and subsequent cooling (or 'residual'). This is important for performance-based fire design for any construction material [12], but it is a quite an open issue in UHPC. As for the testing methods, no specific standards for mechanical tests on UHPC under/after high temperatures exist yet [13]. The compressive strength of UHPCs exposed to high temperatures has been investigated since the 2000s especially in the residual condition, with tests on small samples subjected to pre-established target temperatures and slowly cooled down, to avoid thermal shock. The material strength of UHPC is inevitably investigated

* Corresponding author.
E-mail addresses: scifra@iuav.it (F. Sciarretta), stefano.fava01@gmail.com (S. Fava), mfrancini@buzziunicem.it (M. Francini), luca.ponticelli@vigilfuoco.it (L. Ponticelli), mauro.caciolai@vigilfuoco.it (M. Caciolai), bruno@fzu.edu.cn (B. Briseghella), camillo.nuti@uniroma3.it (C. Nuti).

https://doi.org/10.1016/j.conbuildmat.2021.124608
Received 9 February 2021; Received in revised form 14 August 2021; Accepted 15 August 2021
Available online 2 September 2021

Table 1
Mean quantities of the different components in UHPC mixes, according to [4].

Components	Quantity (kg/m^3)	Density (kg/m^3)	Weight ratio to cement	Weight ratio to binder	Volume fraction
Cement	752	3150	1.00	1.00	0.24
Reactive powders (fly ash, silica fume)	173	2200	0.23		0.08
Inert powders	169	variable	0.22	0.18	–
Silica sand and gravel	887	1500	1.18	0.96	0.60
Superplasticiser (Polycarboxylate ether)	31	1100	0.04	0.03	0.03
Steel fibres	242	7800	0.32	0.26	0.03
PP fibres	2	910	0.003	0.002	0.002
Water	184	1000	0.24	0.20	0.184

on small samples; the material properties must be considered along with the structure's size, loading and environmental conditions.

The paper presents experimental research on the hot and residual compressive strength of two UHPC mixes with polypropylene (PP) and steel fibres at 200 °C. Tests at higher temperature will be carried out in the future on the basis of the present experience. In fact, explosive spalling occurred at 230–290 °C, indicating the need of changes in hybrid fibre composition with respect to what here investigated. The experimental results here presented are discussed in comparison to available literature data on high temperature heating of UHPC samples with reinforcement of PP and PP and steel (i. e. hybrid) fibres. Indications for the future developments are deduced.

The use of PP and steel fibres is frequent in UHPC mixes [14–18]. The addition of PP fibres [19,20] is usual in concrete to withstand high temperatures. PP fibres melt at 165 °C, leaving a network of micro-channels which increases the material permeability, relieving the pore pressure and avoiding the development of high thermal gradients [21,22]. As UHPC releases a high amount of energy at cracking, the addition of steel fibres improves the tensile behaviour of the concrete and can reduce the risk of explosive spalling [23].

Eurocode 2 [24] recommends a minimum PP fibre content of 2 kg/m^3 (circa 0.2% of volume) for the highest grades of HSC; such quantity can be effective for most types of PP fibres in UHPC [25]. According to the American Concrete Institute, a 0.1% of volume in PP fibres is able to significantly reduce spalling [26]; for hydrocarbon fire exposure, the Canadian standard [27] specifies a minimum of 0.3% in volume. On the other hand, research suggests that the quantity of PP fibres required to avoid explosive spalling depends on the UHPC mix design [28]; values from 0.03% to 2% of volume are reported (see Section 3 below).

The evaluation of UHPC compressive strength require tests on small specimens; spalling investigations on UHPC can be performed by heating small specimens in a furnace. While the use of low heating rates can be convenient for strength assessment, high heating rates are usual for spalling investigations measuring the mass loss after the target temperature is attained [21,28–37]. On the other hand, the spalling behaviour of concretes can be investigated by blowtorch exposure of a specified area on a block or wall specimen [38]. As well, research reports the occurrence of explosive spalling during heating cycles on UHPC samples to be mechanically tested under/or after high temperatures [14,15,21,39]. Thus, spalling can impair the mechanical investigations on UHPC.

In the present paper, the tested UHPC mixes behaved in a satisfactory manner at 200 °C; to withstand higher temperatures, the content in PP fibres needs to be increased, while maintaining the highest percentages of steel fibres here adopted.

Table 2
Composition of the tested UHPC mixes (kg/m^3).

ID		Content (kg/m^3) Nanodur Compound 5941	Concrete I 52.5 R	Silica fume	Blast furnace slag	Metakaolin	Super-plasticiser	De-aerator	Sand Dolomia Genova (0–4)	Gravel Dolomia Genova (4–8)	Water	PP fibres	Steel fibres
CLS-A(f_c = 150 N/mm^2)		800	–	80	100	30	40	0.2	750	550	156	2.5	0
													50
													100
CLS-B(f_c = 180 N/mm^2)	B-Lt	1000	–	80	100	30	40	0.5	310	730	165	2.5	0
	B-Bt	700	300	80	100	30	40	1.0	210	850	165	2.5	0
													150
													150

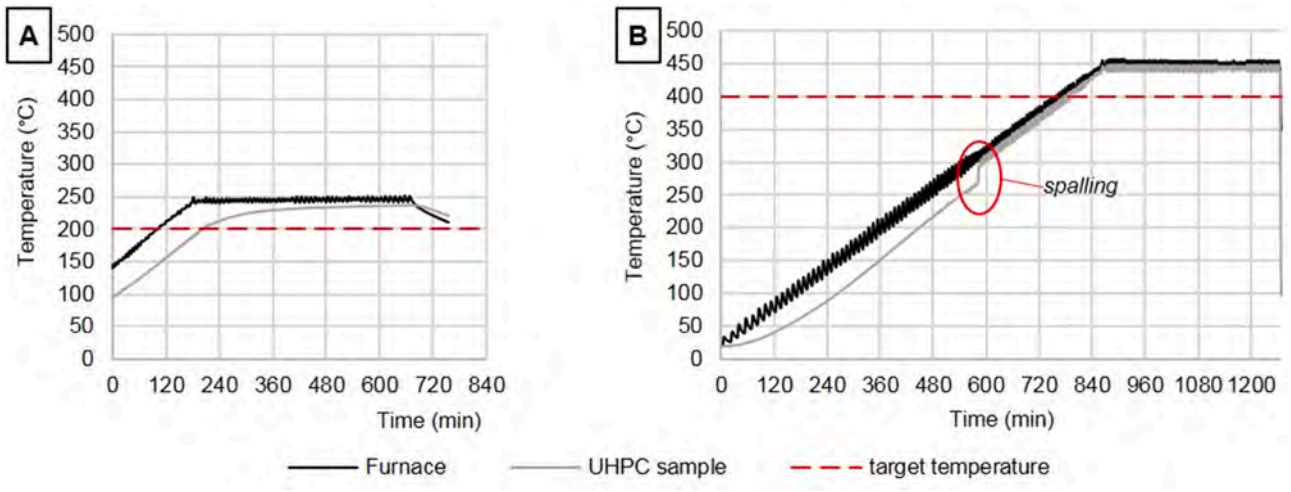

Fig. 1. Temperature recordings of performed thermal cycles: a) target 200 °C; b) target 400 °C.

Table 3
Test results.

Material	age at test (d)	PP fibres (% vol.)	steel fibres (% vol.)	cold tests n. of tests	cold tests f_{cm} (N/mm^2)/CoV	hot tests – 200 °C n. of tests	hot tests – 200 °C $f_{cm,\theta}$ (N/mm^2)/CoV	hot tests – 200 °C %f	residual tests – 200 °C n. of tests	residual tests – 200 °C $f_{cm,\theta,res}$ (N/mm^2)/CoV	residual tests – 200 °C $\%f_{res}$
1	2	3	4	5	6	7	8	9	10	11	12
CLS-A(150 N/mm^2)	28	0.27	0	3	141.9/0.04	3	135.2/0.10	−5%	3	166.8/0.15	+18%
			0.62	3	144.3/0.02	3	135.5/0.17	−6%	3	183.2/0.01	+27%
			1.25	3	146.5/0.03	3	162.2/0.02	+11%	3	199.0/0.01	+36%
	90	0.27	0	3	135.1/0.14	3	123.4/0.15	−9%	3	183.0/0.05	+36%
			0.62	3	149.2/0.04	3	152.4/0.03	+2%	3	186.1/0.05	+25%
			1.25	3	167.4/0.02	3	166.9/0.04	−2%	3	198.1/0.02	+18%
CLS-B-Bt(180 N/mm^2)	28	0.27	0	3	169.8/0.06	1	133.7	−21%	3	190.0/0.01	+12%
			1.9	3	185.1/0.01	3	160.8/0.02	−13%	3	199.9/0.03	+8%
CLS-B-Lt(180 N/mm^2)	90	0.27	0	3	171.6/0.08	0	–	–	3	198.3/0.03	+16%
			1.9	3	177.0/0.02	3	178.1/0.03	+1%	3	224.6/0.03	+27%

1.1. Studies about the effects of PP, steel and hybrid fibre content

Some studies are available to understand the behaviour of UHPC subjected to high temperatures, with the contribution of PP and steel fibres [40–44].

The UHPC matrix has a very compact structure; high temperatures bring on a further increase in compactness, through chemical reactions (decomposition and hydration) [43]. Moreover, the very dense microstructure of UHPC leads to an "internal autoclave" effect, i. e. hydration is entrapped during the heating process, creating a high-temperature and high-pressure environment [15,45,46]. This leads to strength reduction, in absence of the confinement exerted by steel fibre [20,22,36].

The available studies agree about the positive contribution of PP fibres in reducing explosive spalling phenomena, e. g. [18,29,47]; this is in line with experience on normal concrete and HSC. To be effective, fibres must have sufficient length, maintaining a minimal diameter not to affect too much the concrete volume [47]. The escape of steam can be facilitated by the micro-channels and/or micro-cracks generated by the melting of PP fibres, around 165 °C [32]. [38] and [48] enlighten the important role of micro-cracks in connecting the channels network left by melted out fibres, and the good performance of PP fibres 6 mm long, with a diameter of with 0.018 mm (aspect ratio 330). At 360–400 °C, other phenomena can affect the pore pressure (the melted PP releases various volatiles, e. g. pentane, propylene) [49], but such cases have not been experienced in the present research.

The effect of steel fibres on the compressive strength of UHPCs at normal temperature is not as substantial as for NSC and HSC [23]; in fact, the higher stiffness of UHPC impairs the transfer of energy from the matrix to the fibres before cracking, and thus reduces the confinement effect. For the same reasons, the effectiveness of steel fibres in preventing explosive spalling is reduced in UHPCs [15,31,50,51]. Fibres have a bridge effect across cracks, but they may have insufficient stiffness to ensure the integrity of the UHPC specimen; moreover, their strength reduces with temperature [50–52]. Way and Wille [43] observe embrittlement and weakening of steel fibres after exposure to 500 °C and beyond, and complete melting after 800 °C.

Hybrid reinforcement appears to be a need for UHPC exposed at high temperatures. PP and steel fibres together have shown effectiveness in improving the residual strength of UHPC and reducing the explosive spalling hazard [53,30]. In [49], a UHPC with 2% in volume of PP fibres – a very high fibre content, which may impair the material workability – and 1% in volume of steel fibres retains the 70% of the compressive strength after exposure to 1000 °C.

The available tests in literature (reported in Tables A1 and A2 in the Appendix) do not allow to draw exhaustive conclusions about the effects of different dosages and geometry of PP fibres (Section 3); further research seems useful in this field.

2. Experimental investigation

2.1. Materials and testing procedures

The UHCP mixes CLS-A and CLS-B (Table 2) were designed to attain compressive strength of 150 and 180 N/mm^2 respectively, after 28 days. The materials were developed at the R&D Laboratory of Unical s.p.a. (Buzzi Unicem group) in Calenzano (Florence), Italy, where the UHPC specimens were made and left to harden before testing. Then, they were

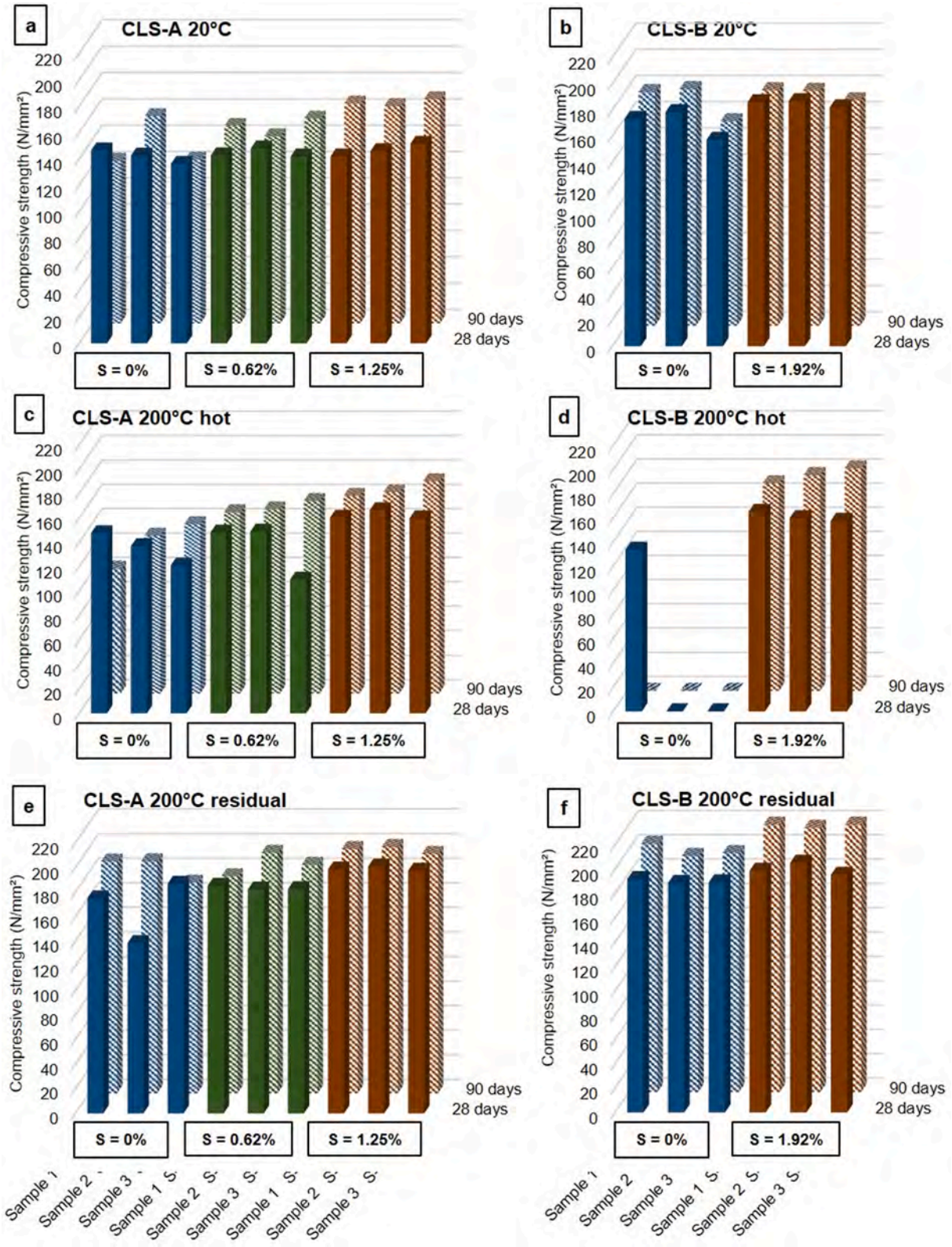

Fig. 2. Results of the single tests (3 samples per age per S) at 20 °C, 200 °C hot and 200 °C residual of CLS-A (a, c, e) and of CLS-B (b, d, f).

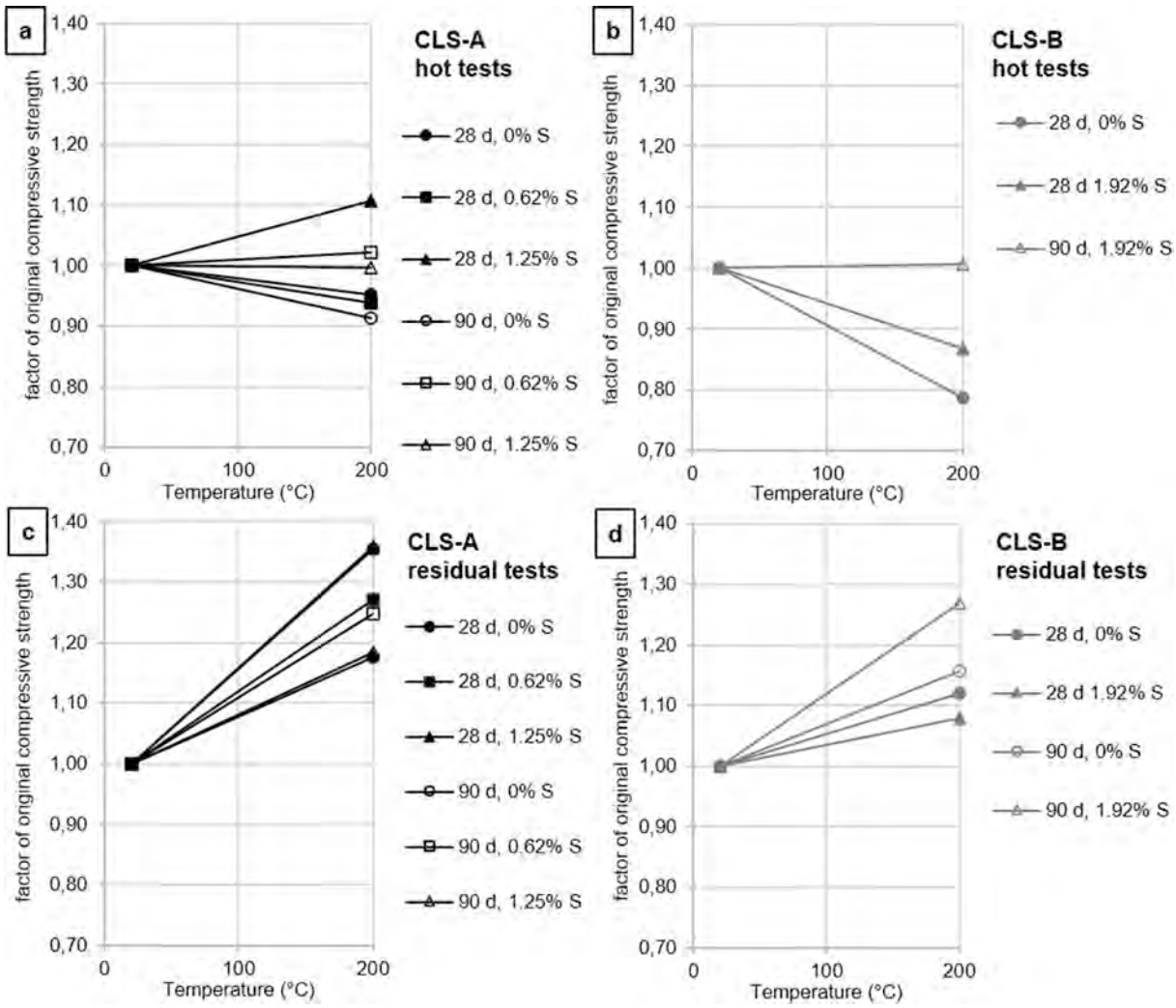

Fig. 3. Trends of temperature-dependent compressive strength of a) CLS-A in hot conditions, b) CLS-A in residual conditions, c) CLS-B in hot conditions, d) CLS-B in residual conditions (d = days).

brought to the Laboratory of Strength of Materials of the National Fire Brigade in Capannelle (Rome), where the heating cycles and mechanical tests in hot conditions were performed.

A single percentage in volume of PP fibres was adopted for all mixes: 0,27%. This dosage was determined according to available recommendations [24–26,54]; the PP fibres have diameter of 0.05 mm and length of 12 mm (aspect ratio: 240). The length is higher than the average values in literature, and the aspect ratio is at the lower bound of literature average (see Table A1 in the Appendix), to affect as less as possible the workability of the fresh material.

CLS-A (150 N/mm2) has a single mix design and three different steel fibre contents, i. e. 0%, 0.62% and 1.25%. CLS-B, which was designed to achieve 180 N/mm2, has two different mixes. The mix indicated with B-Bt (where 'Bt' is for short term) reaches the desired performance in 28 days, while B-Lt (where 'Lt' is for long term) could reach the expected compressive strength only after 90 days. For both mixes, two steel fibre dosages were adopted, i. e. 0% and 1.9% of volume.

For both concretes (A and B), the steel fibres were of two types, i. e. straight fibres of diameter 0.4 mm and length 20 mm (aspect ratio: 50), and hooked fibres of diameter 0.7 mm and length 30 mm (aspect ratio: 43).

The settings of the thermal cycles were established on the grounds of the provisions published by the Italian Council for Research [55]; target temperatures were selected as multiples of 200 °C, with a very low heating rate (0.5 °C/min).

Three samples could be tested for each target. Concrete cubes of 100x100x100 mm were used as samples, according to the capacity of the testing equipment and the very high material strength.

To perform the hot tests, the samples were heated inside a muffle oven (Linn High Therm, model KK-120) and immediately tested according to EN 12390–3 protocol [56], with a RMU C190 hydraulic press. This procedure had been previously adopted at the Fire Brigade Laboratory; the oven and testing machine were moved close to each other and an insulating box was used to keep the sample at the attained temperature, once out of oven, before and during the mechanical test. The box was made of four refractory bricks and rockwool layers, and it was pre-heated in another oven before use, to the same temperature of the sample.

The cold and residual tests were performed at the Material and Structures Research Laboratory of the University of Roma Tre, with a MetroCom Engineering hydraulic press.

Attention was paid to the measurement of the temperature reached by the concrete; literature shows that for Ø100 mm cylindric samples, a<2-hour hold does not allow reaching the target temperature at the core of the sample [14–16,31]. Thermocouples were inserted in some samples to record the core temperature, through a hole of 4 mm diameter and 50 mm depth. The recordings verified that the samples reached the target temperature (Fig. 1a).

The research programme was interrupted after the cycles at target temperature 200 °C, due to explosive spalling of all the samples

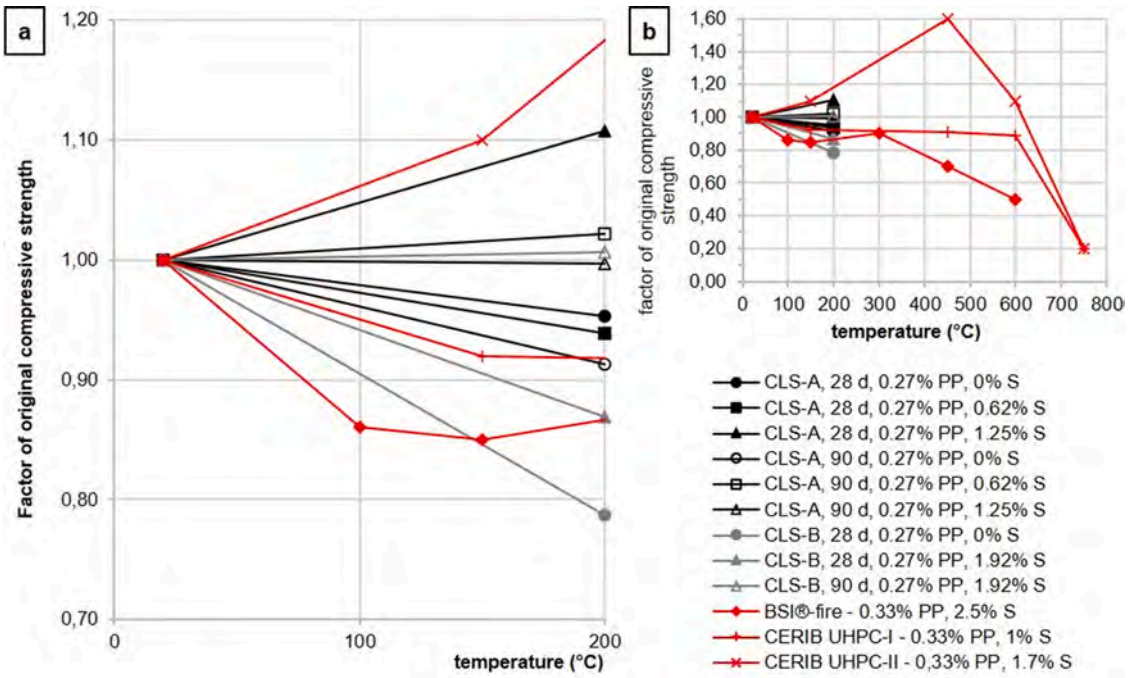

Fig. 4. a) Trends of experimental hot compressive strength, compared to literature data (PP = 0.33%, different S dosages, [17]) b) zoom out.

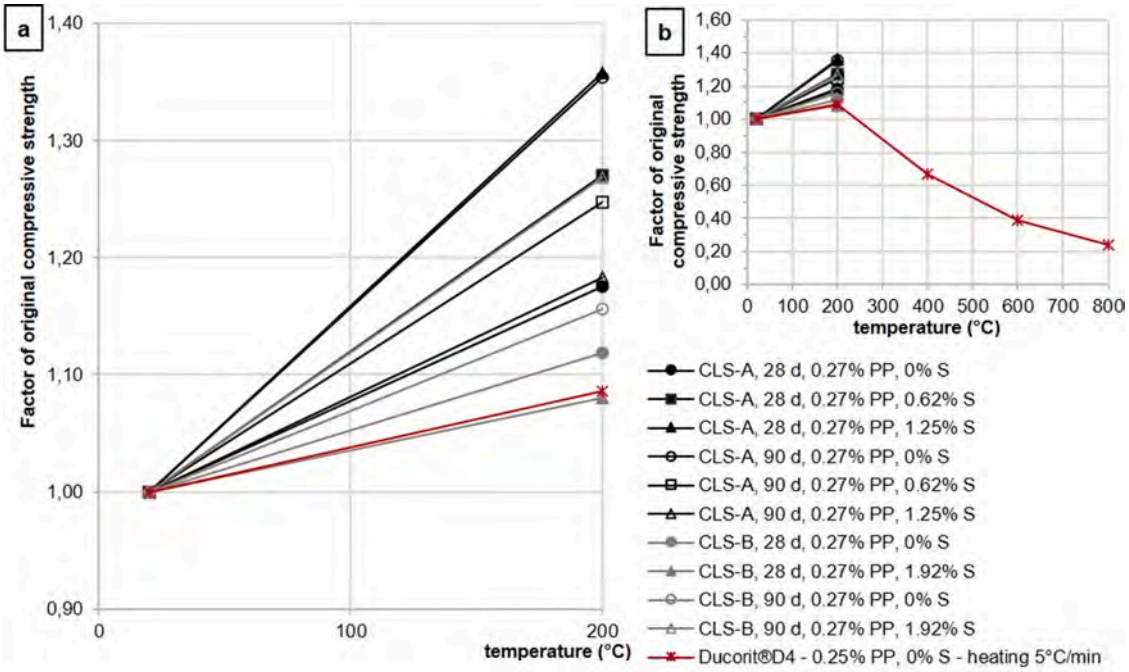

Fig. 5. a) Trends of experimental residual compressive strength, compared to literature datum (PP = 0.25%, S = 0% [21]), b) zoom out.

(Fig. 1b). In detail, the 28-days and the 90-days old samples exploded respectively at temperatures in the range 230–260 °C (CLS-A) and around 290 °C (CLS-B).

2.2. Results

The hot and residual compressive test results, for samples exposed to 200 °C, are commented below in comparison to cold tests (at 20 °C). Henceforth, the volume percentages in PP and steel fibres are abbreviated into PP and S respectively.

Table 3 reports the values of mean compressive strength f_{cm}, $f_{cm,\theta}$, and $f_{cm,\theta,res}$ respectively for cold, hot and residual tests, with the coefficient of variation (CoV, evaluated on the three samples only) and the per cent difference of the property in hot or residual conditions versus the respective cold value (%f and %f_{res}). The strength values of each sample are depicted in histograms in Fig. 2.

Observing the original values (mean values in Table 3, column 6), the 28-days compressive strength of CLS-A shows no relevant variation with the fibre content. On the other hand, at 90-days it increases with steel fibre content, i. e. from 135 to 149, and to 167 N/mm^2, meaning + 3% and + 14% respectively for S = 0.62% and S = 1.25%. The single specimen results in Fig. 2a show a good uniformity at 28 days for each

Table 4
Mechanical tests, from research on UHPCs with PP fibres.

Reference	ID	fibres (%vol) steel	PP	sample (cm)	age at test (d)	hardening means	°C	duration (d)	pre-drying °C	duration (d)	heating (°C/min)	hold (h)
Chen, Yu & Tang 2020 [14]	UHPC-1	0.50	0.03	cylinder ⌀10x20	56	water	N/A	55	–	–	2	0.5
Yang et al. 2019 [16]	HF-CA HF-noCA	1.00	0.15	cube 10	56	water	20	56	105	to desired water content	2	2
Liang et al. 2018 [15]	QS (quartz sand) SS (steel slag)	01.002.00	02.00	cube 5	28	water	90	1	90	1	4	2
Xiong & Liew 2015 [21]	Ducorit®-D4	–	00.100.250.50	cylinder ⌀10x20	28	air (RH 85%)	25–30	28	–	–	530	4
Pimienta et al. 2012 (review paper) [17]	BSI®-fire	2.50	0.33	cylinder ⌀10x30	N/A	N/A	N/A	N/A	N/A	N/A	1	N/A
	Ductal®-AF	1.87	0.46	cylinder ⌀7x14	N/A	N/A	N/A	N/A	N/A	N/A	2	N/A
	Italcementi	–	0.57	cylinder ⌀3.6x11	N/A	N/A	N/A	N/A	N/A	N/A	0.5	N/A
	CERIB_I	1.00	0.33	cylinder ⌀10x30	N/A	N/A	N/A	N/A	N/A	N/A	1	N/A
	CERIB_II	1.71	0.33	cylinder ⌀10x30	N/A	N/A	N/A	N/A	N/A	N/A	1	N/A
	BCV®	2.00	–	cylinder ⌀4x6	N/A	N/A	N/A	N/A	N/A	N/A	3.3	N/A
Burke 2011 [18]	Ductal®-AF	1.94	0.55	cylinder ⌀7.5x15	N/A	steam	90	2	N/A	N/A	N/A	01236
Diederichs & Mertsch 2008 [41]	FIR/LA/PF/H	–	0.06	cylinder ⌀7x19.5	>180	steam	90	2	N/A	N/A	3	1
Felicetti et al. 2000 [42]	RPC (mortar)	2.00	2.00	cubes	N/A	N/A	N/A	N/A	N/A	N/A	1	N/A

steel dosage, and at 90 days except for S = 0%. It may be assumed that the longer curing time increases the bond at the matrix-fibres interfaces, giving a positive contribution to strength.

For CLS-B, both mixes have the same basic strength. They show a moderate strength increase with S = 1.92% for the 28-day old samples (from 170 to 185 N/mm^2, +9%), while for the 90-day old the increase is very slight (from 172 to 177 N/mm^2, +4%). In the latter case, the single specimens indicate some dispersion in the results for S = 0% (Fig. 2b); thus, the limited performance improvement may be disregarded.

As far as it concerns the 200 °C hot tests (Table 3, columns 8 and 9), the steel fibre dosage affects the strength of CLS-A. At 28 days of maturation, the samples with S = 0% and S = 0.62% undergo a very slight reduction in strength (about −5% of mean original strength), while the 1.25% content of steel fibres brings on a moderate increase (+11%). For the former two S percentages, Fig. 2c shows some dispersion in the results of single samples, while data are quite compact in the latter case. At 90 days, the mean strength reduces by −9% for S = 0%, while for both dosages of steel fibres the strength is almost equal to the original (+2% and −2%). Fig. 2c points out a good uniformity in the results of S = 0.62% and S = 1.25%. Thus, at hot conditions (200 °C), the effect of curing time on the strength variation of CLS-A is very limited.

The CLS-B material with PP fibres only (S = 0%) has exhibited a fragile behaviour both in cold and hot conditions. In particular, very violent failures have occurred to the loaded specimens of both CLS-B mixes in hot conditions, so that the machine plates were damaged. The only sample successfully tested, at 28 days (Fig. 2d), resulted in a 21% reduction in strength. It was then decided not to complete the hot tests on the CLS-B samples without steel fibre reinforcement. Such fragile behaviour was assumed to impair any applicability of the material without steel fibre addition.

The hybrid fibre reinforced samples of CLS-B, S = 1.92%, have encountered more ductile failure modes; the mean strength decreases by −13% for the 28-day old samples and undergoes no relevant variation for the 90-day old. Again, Fig. 2d enlightens uniform results in presence of a relevant content in steel fibres.

The residual tests after exposure to 200 °C (Table 3, columns 11 and 12) show increased mean compressive strength, with respect to the original values, for all the samples of both mixes. For CLS-A, the mean strength values at each steel fibre dosage are almost equal for 28- and 90-days old samples. Fig. 2e indicates dispersion in the S = 0% tests at 28 days, while the data are quite compact for the hybrid fibre reinforcement and show a significant strength increase for both steel fibre dosages (+27% and + 36% in the mean values for S = 0.62% and S = 1.25% respectively).

The mean residual strength of CLS-B with S = 1.92% is moderately higher than the original for the 28-days old samples (+8%) and significantly higher (+27%) for the 90-days old samples. This mix with the hybrid reinforcement shows uniform results (Fig. 2f).

On the grounds of the above presented results, trends of the factor of original strength can be plotted in the range 0–200 °C, for the tested UHPC mixes (Fig. 3).

Comparing the results of the present research to literature, Figs. 4 and 5 show the plots of Fig. 3a-d, together with the data of CERIB and BSI®-fire concretes [17], both having PP = 0.33% (for the hot condition) and Ducorit®D4 concrete [21], of PP = 0.25% (for the residual condition).

CERIB UHPC-I and UHPC-II have respectively a compressive strength of 170 N/mm^2 with S = 1%, and 200 N/mm^2 with S = 1.7%. Both have the same types of fibres, i. e. PP fibres 12 mm long, aspect ratio 667, and steel fibres 13 mm long, aspect ratio 81. In hot conditions, the latter has a higher strength gain than the former. BSI®-fire has a strength of 148–165 N/mm^2 with S = 2.5%, with the same PP fibres as the previous two, and steel fibres 20 mm long with aspect ratio 67. This material undergoes a slight reduction in strength in hot conditions. Finally, Ducorit®D4 has a strength of 167 N/mm2 with S = 0%, and PP fibres 13 mm long with aspect ratio 433; it shows a drop (-50%) in the residual strength beyond 200 °C exposure. The graphs' captions report the materials' IDs (see Tables A1 and A2 for other details) and the fibre content

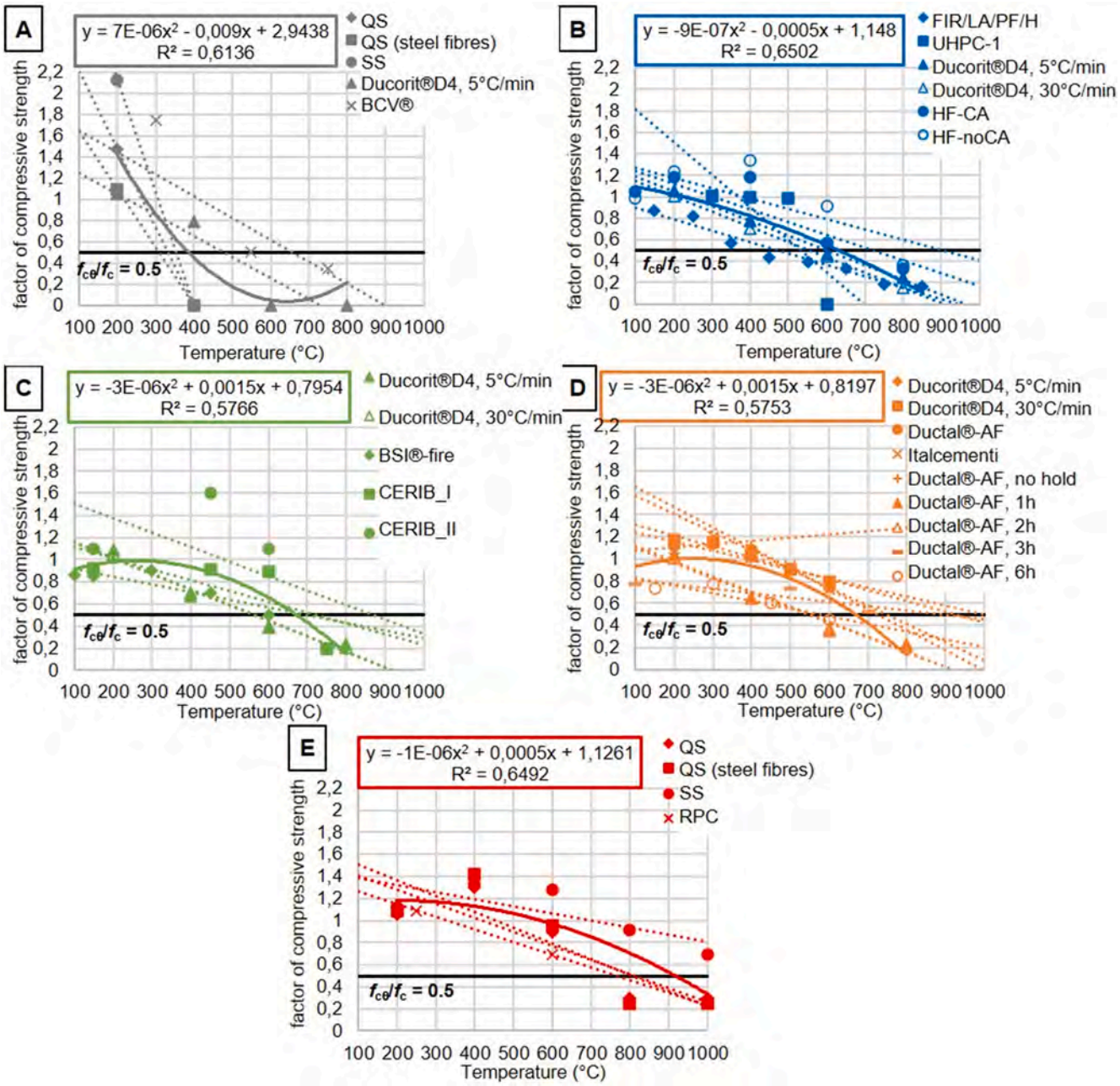

Fig. 6. Linear regression of single $f_{c,\theta}/f_c$-θ series and polynomial regression of all the data set, at variable PP, a) 0%, b) 0.03–0.17%, c) 0.20–0.33%, d) 0.44–0.66%, and e) 2.00%

Table 5
$\theta_{0.5fc}$ values according to single linear and collective polynomial regressions.

PP content range	ID	PP (%)	S (%)	single linear regressions					collective polynomial regression	
				n. data	R^2	$\theta_{0.5fc}$ (°C)	mean	CoV	R^2	$\theta_{0.5fc}$ (°C)
1	**2**	**3**	**4**	**5**	**6**	**7**	**8**	**9**	**10**	**11**
NULL	QS	0	0	2	1.00	330	418	0.34	0.61	385
	QS	0	2.00	2	1.00	310				
	SS	0	0	2	1.00	350				
	Ducorit®D4, 5 °C/min	0	0	4	0.88	445				
	BCV®	0	2.00	4	0.65	655				
LOW	UHPC-1	0.03	0.50	8	0.95	530	632	0.25	0.65	630
	FIR/LA/PF/H	0.06	0	4	0.62	470				
	Ducorit®D4, 5 °C/min	0.10	0	4	0.99	600				
	Ducorit®D4, 30 °C/min	0.10	0	4	1.00	560				
	HF-CA	0.15	1.00	5	0.77	725				
	HF-noCA	0.15	1.00	5	0.52	905				
MEDIUM	Ducorit®D4, 5 °C/min	0.25	0	4	0.96	570	687	0.18	0.58	675
	Ducorit®D4, 30 °C/min	0.25	0	4	0.98	570				
	BSI®-fire	0.33	2.50	5	0,77	695				
	CERIB-I	0.33	1.00	4	0,50	725				
	CERIB-II	0.33	1.70	4	0,32	875				
HIGH	Ductal®-AF	0.46	1.90	2	1.00	900	744	0.24	0.58	675
	Ducorit®D4, 5 °C/min	0.5	0	5	0.96	550				
	Ducorit®D4, 30 °C/min	0.5	0	3	1.00	540				
	Ductal®-AF, no hold	0.55	1.90	5	0.56	–				
	Ductal®-AF, 1 h hold	0.55	1.90	3	0.99	920				
	Ductal®-AF, 2 h hold	0.55	1.90	4	0.96	750				
	Ductal®-AF, 3 h hold	0.55	1.90	4	0.97	995				
	Ductal®-AF, 6 h hold	0.55	1.90	3	0.71	725				
	Italcementi	0.57	0	4	0.82	570				
MAX	QS	2.00	0	5	0.77	810	765	0.10	0.65	918
	QS	2.00	1.00	5	0.74	805				
	SS	2.00	1.00	5	0.57	>1000				
	RPC	2.00	2.00	2	1.00	680				

(% in volume).

In hot conditions at 200 °C (Fig. 4a), the behaviour of CLS-A is intermediate between the two CERIB concretes. As above noted, CLS-A shows a moderate strength increase for the highest dosage in steel fibres (S = 1.25%) at 28 days of age; this is in line with the behaviour of CERIB UHPC II, which displays a strength increase of the same entity at 150 °C.

The decreasing strength of CLS-B at 28 days of age is in line with the behaviour of CERIB UHPC I (S = 1%) and BSI®-fire (S = 2.5%); as noted above, the different CLS-B mix with longer curing time and steel reinforcement S = 1.92% withstands the heating condition without losing strength, which is an intermediate behaviour between CERIB UHPC-I and -II.

In residual conditions (Fig. 5a), CLS-A exhibits a stronger increase in strength than the literature case Ducorit®D4 after 200 °C exposure; the effect of the steel fibre reinforcement (which is absent in the literature case) is evident.

As well (Fig. 5a), the performance of the CLS-B mix at 28 days of age is very similar to Ducorit®D4, regardless of the steel reinforcement. The other mix, which attains the desired strength at 90 days, shows larger strength increases than the literature case, especially with the presence of steel fibres.

Generally, all the cases tested in the present research lie within the envelope of the literature cases. Beyond 200 °C, in hot conditions, the presented reference cases show a stable behaviour up to 600 °C. In residual conditions, the cited case undergoes mechanical decay (Fig. 4b and 5b).

3. Discussion

Literature information and the data of the present research are discussed here below, to provide understanding of the effect of PP fibre percentages (alone and combined with steel fibres into hybrid reinforcement) on the behaviour and properties of UHPCs exposed to high temperatures. In detail, processes of furnace heating on small UHPC samples are taken into consideration. Such processes refer to tests of hot and residual compressive strength tests as well as of spalling.

3.1. Effect of fibres on UHPC residual compressive strength

A collection of literature data allows making considerations about the conditions of effectiveness of PP fibres (with and without steel fibres) in compressive tests on UHPC exposed to high temperatures. Table 4 lists the fibre content, sample types, hardening, pre-drying and testing conditions (i. e. heating rate and hold of the target temperature); N/A denotes unavailable data. The heating rates are generally low, to minimise the risk of spalling (except one study which compares the effects of slow and fast heating [21]). The samples are generally cooled down in air, by turning off the heat and leaving the samples inside the oven; this is due to the need of excluding thermal shock effects. For all the references listed in Table 4, the Appendix provides the concrete mixes (Table A1) and fibres' geometry (Table A2).

On the grounds of the collected references, graphs of the temperature-dependent compressive strength $f_{c,\theta}$ (Fig. 6) allow to individuate possible relationships between residual strength and PP fibre content, and to evaluate the dispersion of results. Based on the PP volume percentages listed in Table 4, the data are subdivided into five intervals, i. e. null (PP = 0%), low (0.03–0.17%), medium (0.20–0.33%), high (0.44–0.66%) and maximum (2%), whose data are plotted in the graphs of Fig. 6. Regression lines are determined for the five groups of $f_{c,\theta}/f_c$ - θ data, following the least square method for each single series; the amount of data for each series and the determination coefficient R^2 for each respective linear regression are listed in Table 5, columns 5 and 6. Then, all the points for each group (null, low, medium, high and max) are collected together; second order polynomial expressions, also shown in Fig. 6, are determined for the collective series (Equations (1) to (5)). The R^2 coefficients are indicated in each subfigure of Fig. 6 and listed in Table 5, column 10.

$$f_{c\theta}/f_c = 7E-06\theta^2 - 0.009\theta + 2.9438 \text{for } PP = 0\% vol. \quad (1)$$

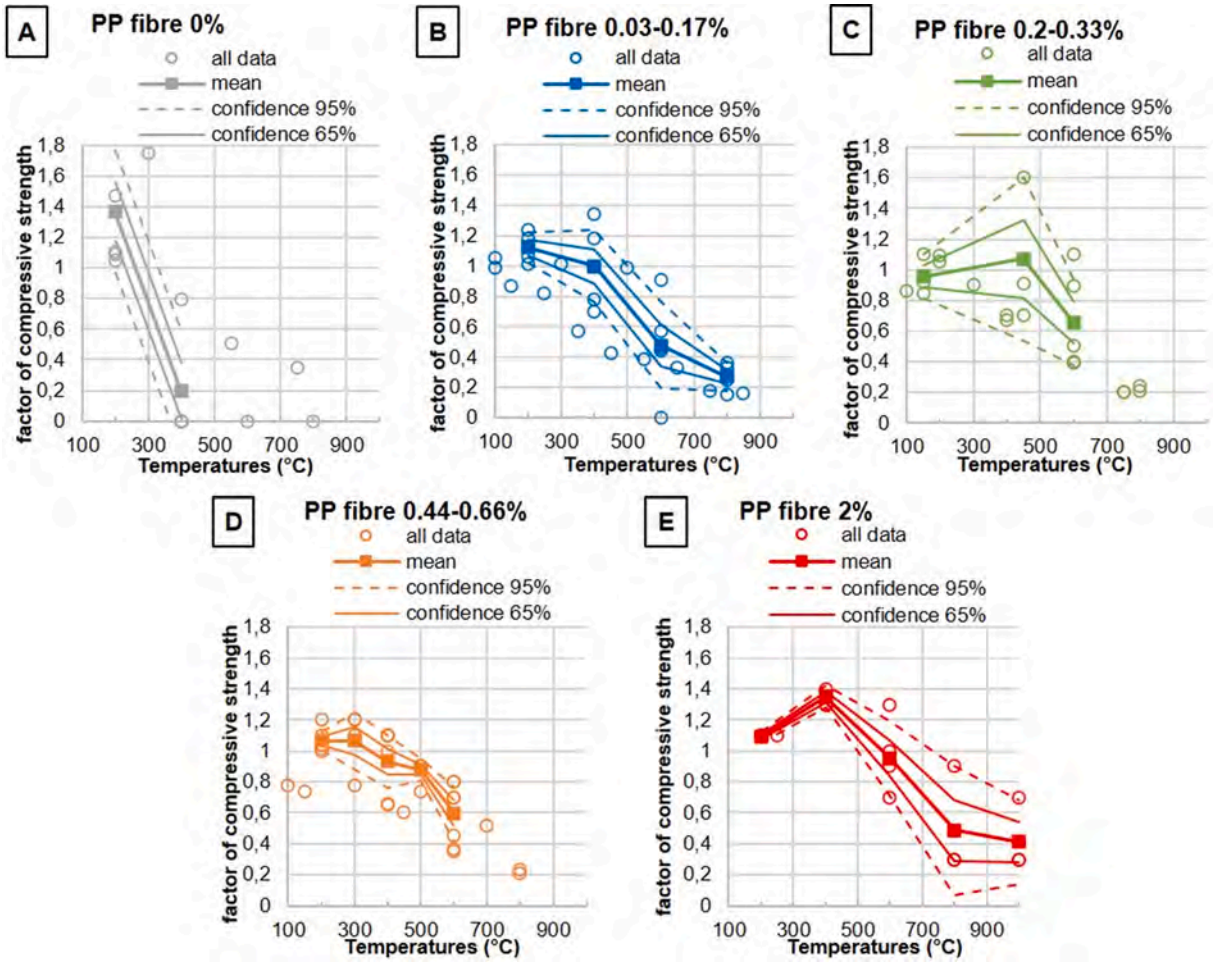

Fig. 7. Mean values and intervals of confidence of 65% and 95% for the considered data sets, a) null PP fibre content, b) low, c) medium, d) high and e) maximum.

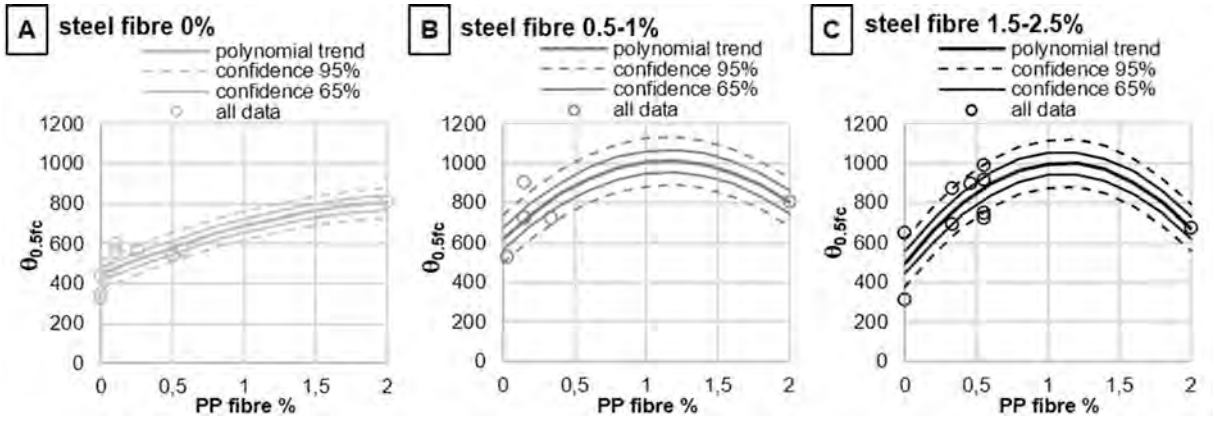

Fig. 8. Mean values and intervals of confidence of 65% and 95% for the considered data sets.

$$f_{c\theta}/f_c = -9E-07\theta^2 - 0.0005\theta + 1.148 \text{ for} PP = 0.03 - 0.17\%\ vol. \quad (2)$$

$$f_{c\theta}/f_c = -3E-06\theta^2 + 0.0015\theta + 0.7954 \text{ for} PP = 0.20 - 0.33\%\ vol. \quad (3)$$

$$f_{c\theta}/f_c = -3E-06\theta^2 + 0.0015\theta + 0.8197 \text{ for } PP = 0.44 - 0.66\%\ vol. \quad (4)$$

$$f_{c\theta}/f_c = -1E-06\theta^2 + 0.0005\theta + 1.1261 \text{ for} PP = 2\%\ vol. \quad (5)$$

In the considered literature, the aspect ratio of PP fibres (reported in Table A2 in the Appendix) is mainly low (167 to 433), as it is in the case of the present research (240, see Section 2 above); five values are higher (667 to 1000) [16,17,30], while in 9 out of 23 cases the aspect ratio of PP fibres is not declared. Concerning the steel fibres, the aspect ratio is between 65 and 83; only two are lower (40, 47) and one is higher (100). In the present research, the aspect ratios of steel fibres (43 and 50) are thus lower than the majority of references.

The temperature after which the residual strength is reduced to the 50% of original value ($\theta_{0.5fc}$) is selected to evaluate the influence of PP parameter. The values of $\theta_{0.5fc}$ are determined by the intersection of the regression lines with $f_{c,\theta}/f_c = 0.5$, as shown in the graphs of Fig. 4. The

Table 6
Spalling tests, from research on UHPCs with PP fibres.

Reference	ID	fibres (%vol) steel	fibres (%vol) PP	nylon	sample (cm)	age (d)	curing means	°C	days	pre-drying °C	pre-drying days	heating (°C/min)	target (°C)	hold (h)
Liu & Zhang 2020 [32]	UHPCPP-1 UHPCPP-2	–	0.22	–	cylinder Ø10x20	>90	airair + water	N/A	20–30	–	–	510	600	1
Li, Tan & Yang 2019 [33]	–	123	0.220.440.66	–	cylinder Ø7.5x15	N/A	lime-saturated water	N/A	27	–	–	~ 60(ISO 834)	945	1
Ozawa et al. 2019 [31]	S IC	2	0.30.5	–	cylinder Ø5x10	N/A	steam	90	2	105	1	~ 60(ISO 834)	842	–
Zhang, Dasari & Tan 2018 [34]	UHPC/O	–	0.33	–	cylinder Ø5x10	28	lime-saturated water	N/A	N/A	–	–	~ 60(ISO 834)	945	1
Sarwar 2017 [28]	UHPC F	1.5	0,22	–	cylinder Ø7.5x15	≥90	steam	90	2	105	≥90	0.2 to 2.45	300 to 700	–
Xiong & Liew 2015 [21]	Ducorit®-D4	–	0.10.2505		cylinder Ø10x20	28	air (RH 85%)	25–30	28	–	–	5	800	4
Choe at al. 2015 [35]	200 MPa 150 MPa	–	0.0750.150.25	0.0750.150.25	cylinder Ø10x20	300	steam	N/A	7	–	–	~ 60(ISO 834)	900	–
Ye at al. 2012 [29]	–	–	12	–	N/A	N/A	N/A	N/A	N/A	N/A	N/A	N/A	400	0.5
Hosser, Kampmeier & Hollmann 2012 [36]	B5Q	2.58	0.080.160.25	–	prism 20x20x60	N/A	N/A	N/A	N/A	N/A	N/A	~ 60(ISO 834)	1000	–
Mindeguia et al. 2007 [37]	BSI®	2.5	0.33	–	cylinder Ø11x22cube 10	28	air–	80–	2–	20 (sealed) 20 (50% RH) pre-heating		~ 500(HCM 180)	1300	3
Heinz, Dehn & Urbonas 2004 [30]	–	2.53.5	0.330.66	–	cylinder Ø10x20	150	water	90	1	20	150	~ 60(ISO 834)	1000	–

linear and nonlinear trends have increasing abscissae of intersection ($\theta_{0.5fc}$) at increasing PP range.

Table 5 lists the values of $\theta_{0.5fc}$ determined in two different ways, i. e. 1) by taking the mean of all the $\theta_{0.5fc}$ values from single linear regressions intersecting $f_{c,\theta}/f_c = 0.5$, and 2) considering the value $\theta_{0.5fc}$ determined by the intersection of each collective polynomial regression line with $f_{c,\theta}/f_c = 0.5$. The values of $\theta_{0.5fc}$ provided by the collective polynomial regressions are mostly on the safe side with respect to the mean value given the single linear regressions, except for the maximum range of PP fibre content. As from Fig. 6C and 6D, the trends for the medium and high range are almost equal. The corresponding $\theta_{0.5fc}$ are also equal, i. e. 675 °C as per Table 5 column 11. This could indicate that the medium range (PP = 0.2 to 0.33%) could be sufficient for substantial improvement in $\theta_{0.5fc}$, but the large dispersion of data should induce some caution. Further performance increase seems obtainable with PP = 2%, which might compromise the workability of the fresh concrete.

Then, the dispersion of the raised data is analysed by determining the intervals of confidence of the 65% and 95% of the values of residual compressive strength (Fig. 7). The mean values and intervals of confidence are calculated for each PP range, at the temperatures for which there are at least three measurements of the residual strength (Table 5, column 5).

It is worth noting that, at any PP range, the values of residual strength have very narrow intervals of confidence at the lowest temperatures (150–200 °C). The graph of examples with null PP (Fig. 7A) shows that a considerable strength increment (a little<40% of the original strength) after exposure at 200 °C could be assumed. However, although data in between are scarce, at 400 °C the 65% interval lies well under the 50% of original strength, being affected by the number of spalling cases before such temperature (zero values).

The low range of PP (0.03–0.17%, Fig. 7B) displays a quite uniform confidence between 200 and 800 °C, showing decrease in residual compressive strength at increasing temperature beyond 200 °C.

It must be noticed that, while in the medium and high ranges (0.20–0.33% and 0.44–0.66%) the regression lines are quite close to each other (Fig. 6C-D), their respective confidence intervals are quite different (Fig. 7C-D). In fact, the dispersion at 450 °C and 600 °C is much larger for the medium than for the high range of PP, underlying the need for further experimental research. Finally, the available data on UHPC with PP = 2.00% (Fig. 7E) show a peculiar increase in residual compressive strength after exposure to 400 °C, with very narrow confidence interval.

The numeric values defining all the lines plotted in Fig. 7 (i. e. mean values, as well as the minimum and maximum values defining the intervals of 95% and 65% confidence) are listed in Table A3 in the Appendix. 2D and 3D graphs are also given in the Appendix (Fig. A1).

Finally, to get a better focus on the effect of hybrid fibre reinforcement, the temperatures after which the material retains only the 50% of original strength ($\theta_{0.5fc}$) are put into relationship with the PP fibre content, at variable steel fibre content (Fig. 8). Three ranges are selected, i. e. S = 0%, 0.5–1% and 1.5–2.5%. Table A4 in the Appendix lists the values plotted with the circle markers in Fig. 8, where second order polynomial regressions are plotted and chosen as a basis for the confidence intervals. The regressions are expressed by Equations (6) to (8), where v_{PP} is the percent value of PP. The determination coefficients R^2 are also indicated.

$$\theta_{0.5fc} = -65.734(v_{PP})^2 + 311.08 v_{PP} + 445.41 \quad [R^2 = 0.69] \text{ for steel fibres } = 0\% \text{ volume} \tag{6}$$

$$\theta_{0.5fc} = -292.4(v_{PP})^2 + 675.98 v_{PP} + 621.35 [R^2 = 0.27] \text{ for steel fibres } = 0.5 - 1\% \text{ volume} \tag{7}$$

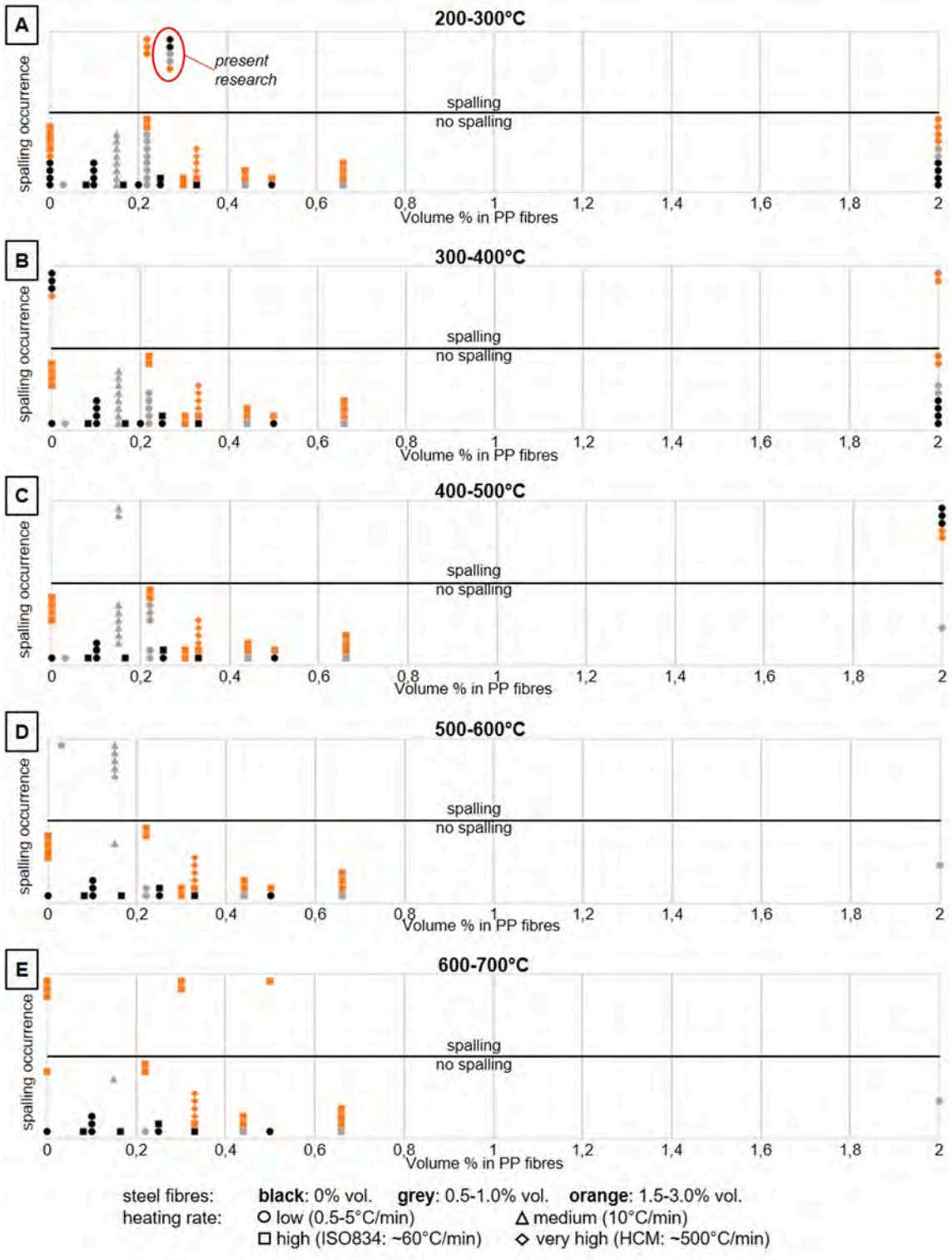

Fig. 9. Spalling occurrence at increasing PP fibre percent in volume, per temperature ranges a) 200–300 °C, b) 300–400 °C, c) 400–500 °C, d) 500–600 °C, e) 600–700 °C.

Table 7
Spalling cases, from research on UHPCs with PP fibres.

Temperature range (°C)	Spalling cases	No spalling cases
200–300	[28] medium PP + high steel fibre content + low heating ratepresent research: medium PP + any steel fibre content + low heating rate	[14–16,21–23,28–31,33,34,36,37]
300–400	[15,36] no fibres + low heating rate[15] maximum PP + high steel fibre content + low heating rate	[14–16,18,21–23,28,31,33,34,36,37]
400–500	[15] maximum PP + null steel fibre content + low heating rate[15] maximum PP + high steel fibre content + low heating rate[16] low PP + medium steel fibre content + medium heating rate	[14–16,18,21–23,28,31,33,34,36,37]
500–600	[14] low PP + medium steel fibre content + low heating rate[16] low PP + medium steel fibre content + medium heating rate	[15,16,18,21,28,31,33,34,36,37]
600–700	[31] zero PP + high steel fibre content + high heating rate[31] low PP + high steel fibre content + high heating rate[31] medium PP + high steel fibre content + high heating rate[31] high PP + high steel fibre content + high heating rate	[15,16,18,21,28,33,34,36,37]

$$\theta_{0.5fc} = -410.18(v_{PP})^2 + 910.3v_{PP} + 497.54 \left[R^2 = 0.59\right] for\ steel\ fibres = 1.5 - 2.5\%\ volume \quad (8)$$

The highest range of S, i. e. 1.5–2.5%, brings on a much higher increase in $\theta_{0.5fc}$ at growing PP fibre content, as it is clear from the three graphs in Fig. 6. The highest content of PP fibres ($v_{PP} = 2.00$), brings the highest benefit to UHPC reinforced with PP only, by taking $\theta_{0.5fc}$ to about 800 °C (Fig. 6A); vice versa, $v_{PP} = 2.00$ appears to give no increase when the reinforcement is hybrid (Fig. 6B-C). However, these observations are based only on a few data related to $v_{PP} = 2.00$, and the lack of data for $0.66 < v_{PP} < 2.00$ impairs any conclusion. Data are scattered, with high R^2 coefficients, therefore further experimental information is needed.

3.2. Effect of fibre content and other parameters on the spalling of UHPC samples

A collection of studies on UHPC spalling, carried on with furnace heating on small samples, is listed in Table 6. Such information is treated jointly with the previously cited studies on temperature-dependent compressive strength (Table 4), to analyse the effects of furnace heating on small samples in terms of spalling occurrence. As a difference from the heating processes related to mechanical tests, in most cases the spalling tests entail much higher heating rates. The target temperatures are very high and the durations at maximum temperature are mostly short (Table 6).

Fig. 9 shows the occurrence of spalling within five temperature ranges, for the cases of Table 6. The graphs exclude the cases which do not mention the spalling temperatures; no spalling is reported beyond 650 °C. The steel fibre dosage is subdivided into three ranges; the different markers denote the heating rate. For every temperature range, the related references, fibre content and heating rates of spalling cases are reported in Table 7.

It can be noticed that spalling can occur in the 200–300 °C and 300–400 °C ranges even at low heating rates. Low and very high contents in PP fibres, as well as steel fibres, can be involved. Within the high PP range (0.44–0.66%), there is only one spalling case, however the total cases are significantly less than at PP < 0.4%.

3.2.1. PP fibre content.

Fig. 10 shows the spalling/no spalling occurrence for all the cases in the considered references, subdivided into hybrid reinforcement (A), and only PP fibres (B), per each of the PP ranges considered above. In detail, for hybrid reinforcement with PP = 0.44–0.66% (Fig. 10A), the data are quite uniform in pointing out an increased effectiveness of the hybrid reinforcement (1 spalling case of 8 total); while for the range of 0.20–0.33% of volume, the good numerosity of data indicates increased effectiveness, but with higher scatter (9 spalling cases in 24 total). On the other hand, for the PP fibres alone, it is difficult to establish an optimum range of fibre volume percentage, since very few data refer to PP > 0.33% (Fig. 10B). In both cases, increasing PP to 2% does not seem to produce commensurate benefits; however, information on PP = 2% is from one research only.

A number of studies ascribe the spalling cases to the effect of vapour pressure inside the pores of the UHPC matrix [14–16,28,29,31], up to PP = 0.66%. On the other hand, for PP = 2%, explosive spalling occurred without vapour emission and was rather due to thermal tension and strain incompatibility between the cement paste and aggregates [15]. It is thus likely that, for very high percentages of PP fibres, a switch occurs from pressure- to stress-driven spalling mechanism, but in-depth investigation should confirm this induction.

Comparing Fig. 10A to 10B, the percentage of spalling cases (histograms on the right) decreases at increasing PP (up to 0.66%) if in combination with steel fibres. At the opposite, when PP fibres are used alone, their benefit – as far as the available data can show – is much reduced beyond the 0.03–0.17% volume range. This might be due to the possible aggravation of pore pressure due to polypropylene decomposition into volatile compounds [49]. Thus, the steel fibres, by playing a complementary role – i. e. bridging the incipient cracks and increasing the material's ductility – can act as a guarantee for the beneficial effect of PP fibres on spalling probability, up to medium and high PP fibre content. Li, Tan and Yang have enlightened this synergetic effect of the fibres [33].

The spalling cases observed in the present research (PP only and hybrid fibre reinforcement, with 0.27% in volume of PP fibres) fit in the not negligible spalling occurrence (i. e. 38%) at PP = 0.20–0.33% reported in the graphs of Fig. 10A-B.

3.2.2. Curing, pre-drying conditions and heating rates.

Some information is available about the effect of different curing conditions for UHPCs subjected to high temperatures. Table 8 resumes the characteristics of the research carried on by Liu and Zhang [32] and Xiong and Liew [21]. The two studies took into account only PP fibre reinforcement, samples of the same type and size, same heating rates and no pre-drying; both of them accounted for wet and dry curing conditions.

Each of the two investigations showed uniform results – all the samples underwent spalling in the former study and no spalling in the latter – across the selected parameters, demonstrating that the curing conditions had negligible effect. While the higher original strength of the concrete in Xiong and Liew's research could have played some role, the relevant differences between the two series of tests could rather be in

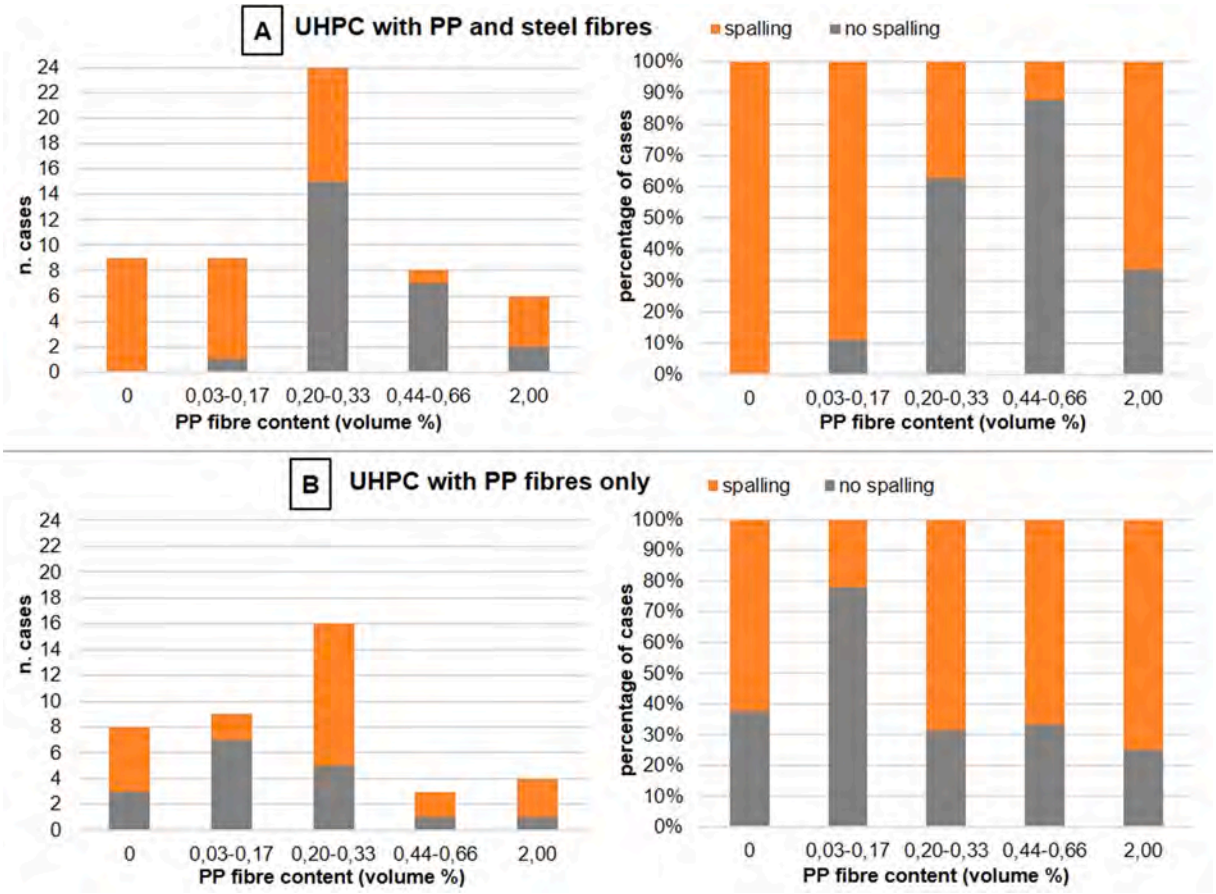

Fig. 10. Spalling occurrence per PP fibre content range, with (a) and without steel fibres (b).

Table 8
Comparison between different experimental results at partially similar conditions.

Ref.	% steel	% PP	sample (cm)	age at testing (d)	material	mix proportions	MPa	curing	pre-drying	Heating rate (°C/min)	target (°C)	hold (h)	result
[32]	0	0.22	cylinder 10x20	>90	UHPCPP-1	cement 1silica fume 0.2silica sand 0.6 superplast. 0.049fine aggreg. 0.6w/c: 0.288	100.1	air (water content 0.02–0.03);air + water 3–4 weeks (water content 0.05)	none	510	600	1	explosive spalling in all cases
					UHPCPP-2	cement 1silica fume 0,2silica powder 0.6 superplast. 0.049w/c: 0.24	116.7						
[21]	0	00.10.250.5	cylinder 10x20	28	Ducorit®-D4	cement, Densit® binder, superplasticiser, fine bauxite aggregatew/mix: 0.076	163	air 25–30 °C, 85% RH;steam 28 °C, 100% RH;sealed specimens + air 25–30 °C, 85%RH	none	5	800	4	no spalling in any case

the materials' mix design. It can be inferred that the high content in silica and ordinary cement could have favoured the onset of spalling [28], while the presence of bauxite aggregate could have significantly improved the fire performance of the basic material [21].

Contrasting points of view are present in literature about the dependency of spalling on the heating rate and initial moisture content of UHPC. Spalling tests mostly envisage very fast heating (Table 6); slow rates (<1 to 5 °C/min) are usually applied in thermal cycles before mechanical tests of residual properties (Table 4), just to avoid the development of excessive thermal gradients. A high heating rate (30 °C/min) could bring on a faster decrease of the residual strength of PP-fibre reinforced UHPC at increasing temperatures [21]. Though a relatively high moisture content has a significant role in facilitating the onset of explosive spalling [16], nonetheless spalling can be experienced at any heating rate and moisture content, e. g. [22,25]. It can be said that the heating rate is of importance as far as it contributes to the pore pressure, which is the predominant trigger of spalling [28,42].

Finally, pre-drying procedures are usually applied to minimise the

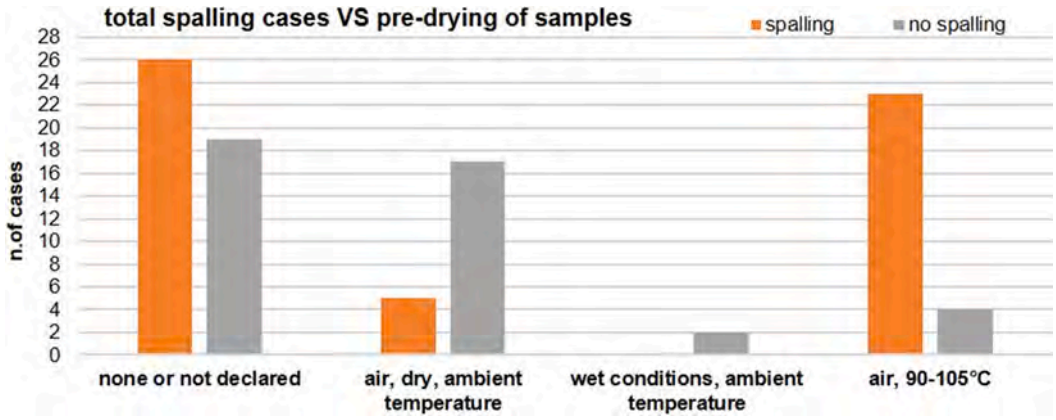

Fig. 11. Total spalling cases vs pre-drying conditions of samples in the considered references.

effect of vapour pressure inside the concrete pores; this allows avoiding the spalling of specimens. However, some research suggests that the pre-drying in oven at 60 to 105 °C could impact the material's microstructure, increasing the concrete's porosity due to capillary stress, cement hydrates desiccation and potential micro-crack generation in relationship with internal thermo-hydric stress [57]. In absence of specific studies, it is worth noting that, in the considered researches, spalling and pre-drying at 90–105 °C in air were often concurrent (23/27 cases), at any volume percent of steel and/or PP fibres (Fig. 11). Air drying at ambient conditions seem to be more beneficial in reducing the likeliness of spalling (17/22 cases).

4. Conclusions

The paper has presented an experimental research aimed at assessing the high temperature behaviour of three UHPC mixes – one (A) of 150 and two (B) of 180 N/mm^2 basic strength – with polypropylene fibres (PP, 0.27% in volume) and steel fibre (S, various percentages in volume from 0% to 1.92%). The compressive strength was measured under and after high temperature exposure. The aspect ratio of the PP fibres (12 mm long) is 240, while steel fibres (of two shapes, length 20 and 30 mm) have aspect ratios of 50 and 43. Results during (hot) and after (residual) exposure to a cycle to 200 °C are given.

- At 200 °C, in hot conditions, CLS-A shows limited strength variations, in line with literature information. At 90 days, the material strength slightly decreases in absence of steel fibres, while it remains at the original level for both steel fibre dosages. At the same condition, the concrete age is not relevant for CLS-A, while the increasing steel fibre dosage brings on a slight performance improvement.
- At the same condition, CLS-B undergoes small strength reductions at 28 days, both for PP-only and hybrid reinforcements; the strength remains at the original levels for the mix which attains the desired strength at 90 days of age.
- After 200 °C, the residual strength of both CLS-A and CLS-B is higher than the original values through all the steel fibre dosages and concrete ages. The contribution of steel fibre is relevant, in fact S = 1.25% and S = 1.92% increases the strength of CLS-A and CLS-B up to about 200 and 225 N/mm^2 respectively.
- After 200 °C, the effect of the steel fibre content on CLS-A is more intense than in hot conditions at the same temperature.
- The benefit of hybrid (PP + steel) fibre content is significant. In the present research, a steel fibre content of 1.25% in volume for CLS-A has increased both hot (+11%) and residual strength (+36%) at 28 days of age. S = 1.92% for CLS-B-Lt (90 days) has increased the residual strength (+27%).
- Available research involving the furnace heating of small UHPC samples encompasses PP = 0–0.66% and 2.00%, and S = 0–3.00%. The results of the present research are confirmed by the available data about mechanical tests, whose dispersion is low at 200 °C.
- Available research shows a considerable dispersion of data about residual compressive strength at PP = 0.20–0.33%, while there is a clear trend for PP = 0.44–0.66%. This is a good indication for the developments of the present research; the increase in PP percentage to 0.44–0.66% - with adequate aspect ratio of fibres, i. e. 200–300 - is foreseen.
- Available literature points at hybrid reinforcement with values of S higher than 1%, like the upper values considered in the present research. This is as well an indication for future investigations.
- Beyond 200–400 °C, as literature reports, the residual compressive strength of UHPC decreases; the trend depends on the PP fibre dosages. This is especially clear by observing $\theta_{0.5fc}$ (the temperature at which the strength is reduced to 50%). A very high PP fibre content (2%) shows significant benefit, but such a high dosage should account for possible issues of fresh material's workability. This also indicates an important field for future investigations.
- About the heating of UHCP samples with hybrid fibre contents, literature reports the occurrence of spalling at very different temperatures, from 200 to 300 °C (like it happened in the present research) on. For higher temperatures, up to 600–700 °C, cases of disruptive spalling involved any range of steel and PP fibre percentage; high fibre percentages seem worth investigation.

Declaration of Competing Interest

The authors declare that they have no known competing financial interests or personal relationships that could have appeared to influence the work reported in this paper.

Acknowledgements

The authors warmly thank the Italian Fire Brigade, Buzzi Unicalcestruzzi, Federbeton (Italy) for financial support for "Seismic Behaviour of Integral Bridges" and DPC-ReLUIS consortium for the financial support within the framework of the 2014-2018 and 2019-2021 Research Projects. The research was supported by the National Natural Science Foundation of China (Grant No. 51778148).

Appendix A. Supplementary data

Table A1
Tests on UHPCs with PP fibres: UHPC mix design.

Reference	Tests	Country	ID	p	c	sf	sp	qp	fl	s	va	st	bl	g	mk	ss	ca	fa	w/c	f_c (N/mm2)
present research	M	Italy	CLS-A	x		x				x			x		x		x	x	0.195*	150
			CLS-B	x		x				x			x		x		x	x	0.165*	200
Chen, Yu & Tang 2020 [14]	M	Taiwan	UHPC-1		x	x	x			x	x							x	0.195	156
Liu & Zhang 2020 [32]	S	China	UHPCPP-1		x	x				x						x		x	0.29	100
			UHPCPP-2		x	x				x						x		x	0.29	117
Yang et al. 2019 [16]	M, S	China	HF-CA		x	x			x				x				x	x	0.18	157
			HF-noCA		x	x			x				x					x	0.18	145
Li, Tan & Yang 2019 [33]	S	Singapore	–		x	x				x						x		x	0.2*	150
Ozawa et al. 2019 [31]	S	Japan	S	x						x								x	0.14*	213
			IC	x						x								x	0.14*	213
Liang et al. 2018 [15]	M	Australia -	quartz sand		x	x			x	x								x	0.21	112
		China	steel slag		x	x			x	x		x							0.21	90
Zhang, Dasari & Tan 2018 [34]	S	Singapore	UHPC/O		x	x				x						x		x	0.2*	160
Sarwar 2017 [28]	S	USA	UHPC F		x	x				x			x			x	x	x	0.14	165
Xiong & Liew 2015 [21]	M, S	Singapore	Ducorit®-D4	x															0.076*	167
Choe at al. 2015 (PP + nylon fibres) [35]	S	USA	200 MPa		x	x				x			x	x		x	x	x	0.227	205
			150 MPa		x	x				x			x	x		x	x	x	0.23	149
Pimienta et al. 2012 (review paper) [17]	M	France	BSI®-fire	x															0.19*	148–165
		France	Ductal®-AF	x															0.14*	160
		Italy	Italcementi	x														x	0.31*	121
		France	CERIB_I	N/A																170
		France	CERIB_II	N/A																200
		France	BCV®	x															0.104*	155
Ye at al. 2012 [29]	S	China	–	x	x												x	x	0.22	N/A
Hosser, Kampmeier & Hollmann 2012 [36]	S	Germany	B5Q		x	x		x		x							x	x	0.2	N/A
Burke 2011 [18]	M	USA	Ductal®-AF	x						x	x								0.186	142
Diederichs & Mertsch 2008 [41]	M	Germany, Finland	FIR/LA/PF/H		x	x				x							x	x	0.2	158
Mindeguia et al. 2007 [37]	S	France	BSI®	x						x									0.2*	N/A
Heinz, Dehn & Urbonas 2004 [30]	S	Germany	–		x	x				x								x	0.18	180
Felicetti et al. 2000 [42]	M	Italy - UK	RPC (mortar)		x	x												x	0.18	160

M: mechanical tests, S: spalling tests; pr: premix, c: cement, sf: silica fume, sp: silica powder, qp: quartz powder, fl: fly ash, s: superplasticizer, va: viscous agent, st: steel slag, bl: blast furnace slag, g: gypsum, mk: metakaolin, ss: silica sand, ca: coarse aggregates, fa: fine aggregates; w/c: water-concrete ratio, *) water/premix ratio.

Table A2
Fibres' geometry for the considered references.

study	steel fibres				PP fibres				type of tests
	% vol.	∅ (mm)	L (mm)	AR	% vol.	∅ (mm)	L (mm)	AR	
Present research	0.0 0.64 1.28 1.92	0.4 0.7	2030	5043	0.27	0.05	12	240	M
Chen. Yu and Tang (2020) [14]	0.5	0.2	13	65	0.03	0.05	12	240	M
Liu & Zhang (2020) [32]	–	–	–	–	0.22	0.06	10	167	S
Yang et al. (2019) [16]	1.0	0.2	16	80	0.15	0.02	19	950	M, S
Li. Tan & Yang (2019) [33]	0 1.0 2.0 3;0	0.22	13	59	0 0.22 0.44 0.66	0.03	12	400	S
Ozawa et al. (2019) [31]	2.0	0.2	15	75	0 0.3 0.5	0.042	12	286	S
Zhang, Dasari & Tan (2018) [34]	–	–	–	–	0 0.33	0.033	12	364	S
Liang et al. (2018) [15]	0.0 1.0 2.0	0.12	10	83	0.0 2.0	0.031	10	323	M. S
Sarwar (2017) [28]	1.5	N/A	N/A	N/A	0.22	N/A	N/A	N/A	S
Xiong & Liew (2015) [21]	–	–	–	–	0 0.10 0.25 0.50	0.03	13	433	M. S
Choe et al. (2015) [35]	–	–	–	–	0.075 0.15 0.25	N/A	N/A	N/A	S
Burke (2011) [18]	1.94	0.2	14	70	0.55	N/A	N/A	N/A	M
Pimienta et al. (2012) - BSI®-fire [17]	2.5	0.3	20	67	0.33	0.018	12	667	M
Pimienta et al. (2012) - Ductal®-AF [17]	1.87	0.2	13	65	0.46	N/A	N/A	N/A	M
Pimienta et al. (2012) – Politecn.-Italcementi [17]	–	–	–	–	0.57	0.02	20	1000	M
Pimienta et al. (2012) – CERIB UHPC_I [17]	1.0	0.16	13	81	0.33	0.018	12	667	M
Pimienta et al. (2012) – CERIB UHPC_II [17]	1.7	0.16	13	81	0.33	0.018	12	667	M
Pimienta et al. (2012) - BCV® [17]	2.0	0.175	12.7	73	–	–	–	–	M
Ye et al. (2012) [29]	–	–	–	–	0.1 0.2	N/A	19	N/A	S
Hosser, Kampmeier & Hollmann (2012) [36]	2.6	0.19	9	47	0 0.082 0.0165 0.25	N/A	N/A	N/A	S
Diederichs & Mertsch (2008) [41]	–	–	–	–	0.06	N/A	N/A	N/A	M
Mindeguia et al. (2007) [37]	2.5	0.3	20	67	0.033	N/A	N/A	N/A	S
Heinz. Dehn & Urbonas (2004) [30]	2.5 3.5	0.15	6	40	0 0.33 0.66	0.016	4.9	306	S
Felicetti et al. (2000) [42]	2.0	0.16	16	100	2.0	N/A	N/A	N/A	M

∅ : diameter, L: length, AR: aspect ratio (L/Ø).

Table A3
Mean values and intervals of confidence for the collected data (graphs $f_{c,\theta}/f_c$ - θ).

PP fibre quantity(% vol.)	°C	n. data	mean $f_{c\theta}$ (N/mm^2)	standard deviation	confidence 95%		confidence 65%	
					max	min	max	min
0 – NULL	200	5	1,366	0,454	1,764	0,968	1,556	1,176
	400	4	0,198	0,395	0,585	−0,190	0,382	0,013
0.03–0.17 - LOW	200	4	1,123	0,106	1,226	1,019	1,172	1,073
	400	5	1,000	0,268	1,235	0,765	1,112	0,888
	600	5	0,476	0,326	0,762	0,190	0,612	0,340
	800	4	0,273	0,094	0,365	0,180	0,316	0,229
0.20–0.33 - MEDIUM	150	3	0,957	0,129	1,103	0,811	1,026	0,887
	450	3	1,070	0,471	1,603	0,537	1,324	0,816
	600	5	0,656	0,321	0,937	0,375	0,790	0,522
0.44–0.66 - HIGH	200	5	1,066	0,069	1,126	1,006	1,095	1,037
	300	4	1,065	0,192	1,253	0,877	1,155	0,975
	400	6	0,932	0,216	1,104	0,759	1,014	0,849
	500	5	0,878	0,079	0,947	0,809	0,911	0,845
	600	5	0,599	0,199	0,773	0,424	0,682	0,516
2.00% - MAXIMUM	200	3	1,090	0,030	1,124	1,056	1,106	1,074
	400	3	1,350	0,062	1,421	1,279	1,384	1,316
	600	4	0,953	0,245	1,193	0,712	1,067	0,838
	800	3	0,487	0,367	0,902	0,071	0,685	0,288
	1000	3	0,413	0,241	0,686	0,141	0,543	0,283

Table A4
Mean values and intervals of confidence for the collected data (graphs $\theta_{0.5fc}$ - v_{PP}).

steel %	ID	PP%	steel %	$T_{50\%fc}$	mean	standard deviation	interval of confidence 95%		interval of confidence 65%	
							max	min	max	min
0%	QS	0	0	330	530.4	125.3	601.3	459.5	564.2	496.6
	SS	0	0	350						
	Ducorit®D4, 5 °C/min	0	0	445						
	FIR/LA/PF/H	0.06	0	470						
	Ducorit®D4, 5 °C/min	0.10	0	600						
	Ducorit®D4, 30 °C/min	0.10	0	560						
	Ducorit®D4, 5 °C/min	0.25	0	570						
	Ducorit®D4, 30 °C/min	0.25	0	570						
	Ducorit®D4, 5 °C/min	0.5	0	550						
	Ducorit®D4, 30 °C/min	0.5	0	540						
	Italcementi	0.57	0	570						
	QS	2.00	0	810						
0.5–1.5%	UHPC-1	0.03	0.50	530	738	137.8	858.8	617.2	795.6	680.4
	HFCA	0.15	1.00	725						
	HFnoCA	0.15	1.00	905						
	CERIB-I	0.33	1.00	725						
	QS	2.00	1.00	805						
1.5–2.5%	QS	0	2.00	310	750.5	193.8	870.6	630.3	807.8	693.2
	BCV®	0	2.00	655						
	BSI®-fire	0.33	2.50	695						
	CERIB-II	0.33	1.70	875						
	Ductal®-AF	0.46	1.90	900						
	Ductal®-AF	0.55	1.90	920						
	Ductal®-AF	0.55	1.90	750						
	Ductal®-AF	0.55	1.90	995						
	Ductal®-AF	0.55	1.90	725						
	RPC	2.00	2.00	680						

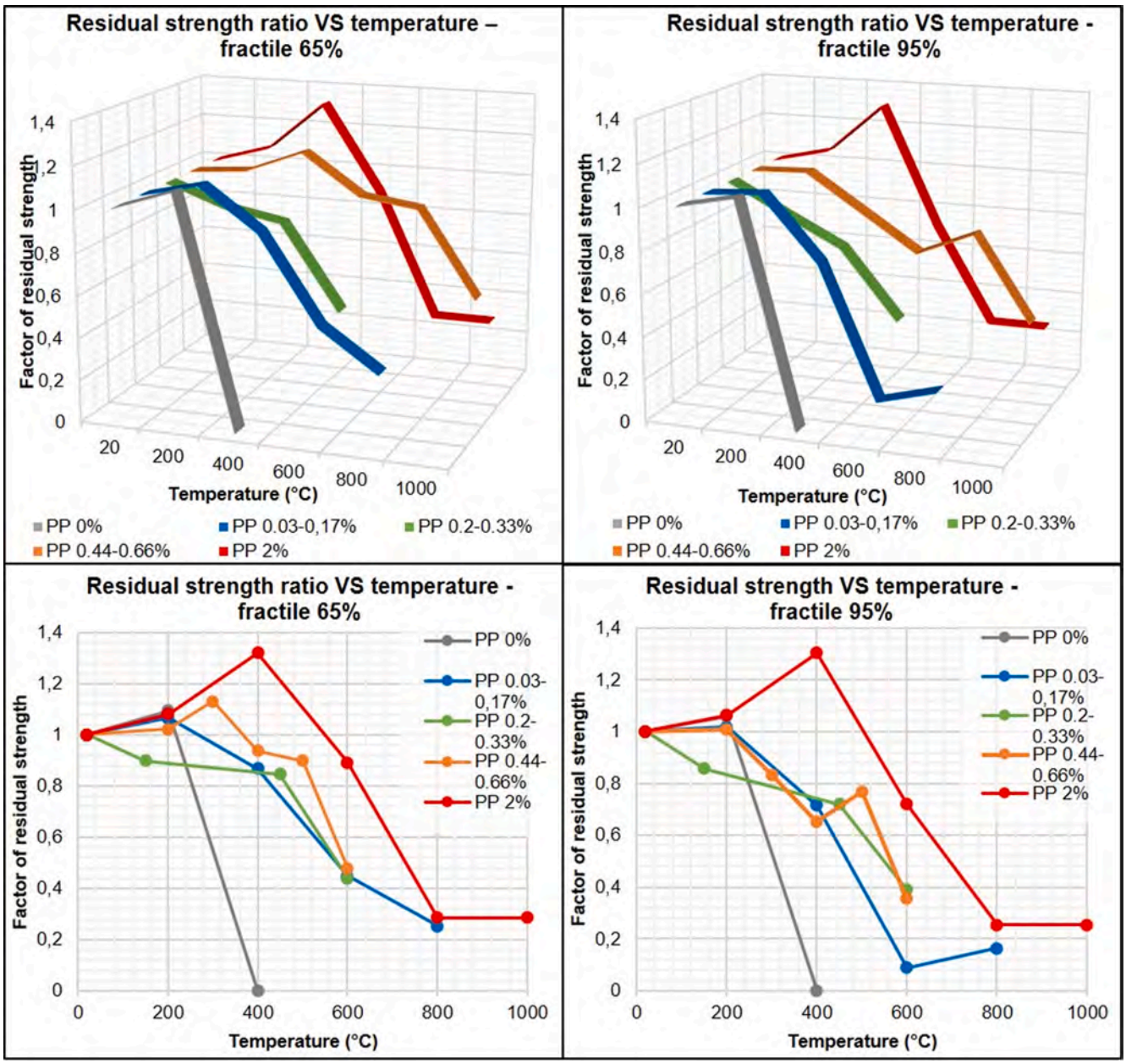

Fig. A1. 2D and 3D graphs of the residual strength ratio vs temperature of exposure.

References

[1] B. Graybeal, Ultra High Performance concrete. Federal Highway Administration Research and Technology, publication n° FHWA-HRT-11-038, 2011.

[2] Recommendations (2013).

[3] V. Perry, What really is Ultra-High Performance Concrete? Towards a global definition, in: C. Shi, B. Chen (Eds.), Proceedings of 2nd International Conference on UHPC Materials and Structures, Fuzhou, 2018.

[4] T. Stengel, P. Schiessl, 22 – Life cycle assessment (LCA) of Ultra-High Performance Concrete (UHPC) structures, in: F. Pacheco-Torgal, L.F. Cabeza, J. Labrincha, A. de Magalhães (Eds.), Eco-efficient Construction and Building Materials, Woodhead Publishing Ltd., 2014, pp. 528–564, https://doi.org/10.1533/9780857097729.3.528.

[5] H.G. Russell, B. Graybeal, Ultra-high performance concrete: a state-of-the-art-report for the bridge community, Federal Highway Administration Research and Technology, publication n° FHWA-HRT-13-060 (2013).

[6] E. Denarié, E. Brühwiler, Structural rehabilitations with ultra-high performance fibre reinforced concretes (UHPFRC), Restor. Build. Monum. 12 (5/6) (2006) 453–468.

[7] J. Xue, D. Lavorato, A.V. Bergami, C. Nuti, B. Briseghella, G.C. Marano, T. Ji, I. Vanzi, A.M. Tarantino, S. Santini, Severely damaged reinforced concrete circular columns repaired by turned steel rebar and high-performance concrete jacketing with steel or polymer fibers, Appl. Sci. 8 (9) (2018) 1671, https://doi.org/10.3390/app8091671.

[8] M. Empelmann, M. Teutsch, G. Steven, Expanding the application range of RC-columns by the use of UHPC, in: J.C. Walraven, D. Stoelhorst (Eds.), Tailor Made Concrete Structures, Taylor and Francis Group, London, 2008, pp. 461–468.

[9] T. Stengel, P. Schiessl, Sustainable construction with UHPC – from life cycle inventory data collection to environmental impact assessment, in: E. Fehling, M. Schmidt, S. Stürwald (Eds.), Proceedings of the 2nd International Symposium on Ultra High Performance Concrete, Kassel, 2008, pp. 461-468.

[10] M. Rebentrost, G. Wight, Experience and applications of ultra-high performance concrete in Asia, in: E. Fehling, M. Schmidt, S. Stürwald (Eds.), Proceedings of the 2nd International Symposium on Ultra High Performance Concrete, Kassel, 2008, pp. 461-468.

[11] J. Xue, B. Briseghella, F. Huang, C. Nuti, H. Tabatabai, B. Chen, Review of ultra-high performance concrete and its application in bridge engineering, Construction and Building Materials 260 (2020) 119844, https://doi.org/10.1016/j.conbuildmat.2020.119844.

[12] F. Sciarretta, Modeling of mechanical damage in traditional brickwork walls after fire exposure, Advanced Materials Research 919-921 (2014) 495-499. https://doi.org/10.4028/www.scientific.net/AMR.919-921.495.

[13] Fire resistance – Tests for thermophysical and mechanical properties of structural meterials at elevated temperatures for fire engineering design. ISO/TR 15655, International Standard Organisation, 2020.

[14] D. Cree, P. Pliya, M.F. Green, A. Noumowé, Thermal behaviour of unstressed and stressed high strength concrete containing polypropylene fibers at elevated temperature, JSFE 8 (4) (2017) 402–417.
[15] N. Yermak, P. Pliya, A.-L. Beaucour, A. Simon, A. Noumowé, Influence of steel and/or polypropylene fibres on the behaviour of concrete at high temperature: Spalling, transfer and mechanical properties, Construction and Building Materials 132 (2017) 240–250.
[16] M.-X. Xiong, J.Y. Richard Liew, Spalling behavior and residual resistance of fibre reinforced Ultra-High performance concrete after exposure to high temperaturesSpalling behavior and residual resistance of fibre reinforced Ultra-High performance concrete after exposure to high temperatures, Mater. construcc. 65 (320) (2015) e071, https://doi.org/10.3989/mc.2015.v65.i32010.3989/mc.2015.00715.
[17] Y. Li, K.H. Tan, in: Effects of polypropylene and steel fibers on permeability of ultra-high performance concrete at hot state, Princeton University, 2016, pp. 145–152.
[18] I.L. Larsen, R.T. Thorstensen, The influence of steel fibres on compressive and tensile strength of ultra high performance concrete: A review, Construction and Building Materials 256 (2020) 119459, https://doi.org/10.1016/j.conbuildmat.2020.119459.
[19] H.-J. Chen, Y.-L. Yu, Ch.-W. Tang, Mechanical properties of Ultra-High Performance Concrete before and after exposure to high temperatures. Mater. 13 (2020), 770. https://doi.org/10.3390/ma13030770.
[20] X. Liang, C. Wu, Y.u. Su, Z. Chen, Z. Li, Development of ultra-high performance concrete with high fire resistance, Construction and Building Materials 179 (2018) 400–412.
[21] J. Yang, G.-F. Peng, J. Zhao, G.-S. Shui, On the explosive spalling behavior of ultra-high performance concrete with and without coarse aggregate exposed to high temperature, Construction and Building Materials 226 (2019) 932–944.
[22] Felicetti, P. Bamonte, P. G. Gambarova, Literature review on the behaviour of UHPFRC at high temperature, in: M. Schmidt, E. Fehling, C. Glotzbach, S. Frölich, S. Piotrowski (Eds.), Proceedings of Hipermat – 3rd International Symposium on UHPC and Nanotechnology for High Performance Construction Materials, Kassel, 2012, pp. 549-556.
[23] B. T. Burke, Residual strength of Ultra-High Performance Concrete after exposure to elevated temperatures, Master's thesis, University of Connecticut, 2011. URL: https://opencommons.uconn.edu/gs_theses/44.
[24] Eurocode 2: Design of concrete structures – Part 1-2: General rules – Structural fire design, Comité Européen de Normation, EN 1992-1-2, 2004.
[25] F. Lu, M. Fontana, in: Effects of polypropylene fibres on preventing concrete spalling in fire, Princeton University, 2016, pp. 241–248.
[26] Ultra-high performance Concrete: an Emerging Technology Report. American Concrete Institute, C-239 Committee, PRC-239-18, 2018.
[27] Concrete materials and methods of concrete construction/Test methods and standard practices for concrete. CSA Group, A23.1/A23.2, 2019.
[28] M. A. Sarwar, Characterizing temperature-induced strength degradation and explosive spalling in ultra-high performance concrete. Civil Engineering MS thesis, Michigan State University, 2017. URL: https://d.lib.msu.edu/etd/6756.
[29] Hao-wen Ye, Nai-qian Feng, Yan Ling-hu, Zhi-wei Ran, Li-xun Lin, Shi-kun Qi, Yi Dong, Research on Fire Resistance of Ultra-High-Performance Concrete, Advances in Materials Science and Engineering 2012 (2012) 1–7.
[30] D. Heinz, F. Dehn, L. Urbonas, Fire resistance of Ultra High Performance Concrete (UHPC) – Testing of laboratory samples and columns under load, in: M. Schmidt, E. Fehling, C. Geisenhanslüke (Eds.), Proceedings of the International Symposium on Ultra High Performance Concrete, 2004, pp. 703–715.
[31] Mitsuo Ozawa, Sirjana Subedi Parajuli, Yuichi Uchida, Bo Zhou, Preventive effects of polypropylene and jute fibers on spalling of UHPC at high temperatures in combination with waste porous ceramic fine aggregate as an internal curing material, Construction and Building Materials 206 (2019) 219–225.
[32] Jin-Cheng Liu, Zhigang Zhang, Neural network models to predict explosive spalling of PP fiber reinforced concrete under heating, Journal of Building Engineering 32 (2020) 101472, https://doi.org/10.1016/j.jobe.2020.101472.
[33] Ye Li, Kang Hai Tan, En-Hua Yang, Synergistic effects of hybrid polypropylene and steel fibers on explosive spalling prevention of ultra-high performance concrete at elevated temperature, Cement and Concrete Composites 96 (2019) 174–181.
[34] Dong Zhang, Aravind Dasari, Kang Hai Tan, On the mechanism of prevention of explosive spalling in ultra-high performance concrete with polymer fibers, Cement and Concrete Research 113 (2018) 169–177.
[35] Gyeongcheol Choe, Gyuyong Kim, Nenad Gucunski, Seonghun Lee, Evaluation of the mechanical properties of 200 MPa ultra-high-strength concrete at elevated temperatures and residual strength of column, Construction and Building Materials 86 (2015) 159–168.
[36] D. Hosser, B. Kampmeier, D. Hollmann, Behaviour of Ultra High Performamce Concrete (UHPC) in case of fire, in: M. Schmidt, E. Fehling, C. Glotzbach, S. Frölich, S. Piotrowski (Eds.), Proceedings of Hipermat – 3rd International Symposium on UHPC and Nanotechnology for High Performance Construction Materials, Kassel, 2012, pp. 573-582.
[37] J. C. Mindeguia, P. Pimienta, A. Simon, N. Atif, Experimental and numerical study of an UHPFRC at very high temperature, in: F. Toutlemonde, K. Sakai, O. E. Gjorv, N. Banthia (Eds.), Proceedings of CONSEC'07, Concrete Under Severe Conditions: Environment and Loading, Tours, 2007, ID 175.
[38] L. Missemer, E. Ouedraogo, Y. Malecot, C. Clergue, D. Rogat, Fire spalling of ultra-high performance concrete: From a global analysis to microstructure investigations, Cement and Concrete Research 115 (2019) 207–219.
[39] Ch. Kahanji, F. Ali, A. Nadjai, in: Experimental study of ultra-high performance fibre reinforced concrete under ISO 834 fire, Princeton University, 2016, pp. 165–173.
[40] C. Nuti, J. Xue, S. Fava, P. Castelli, L. Euzor, M. Francini and L. Ponticelli, Experimental behavior of UHPC under fire action, in: C. Shi, B. Chen (Eds.), Proceedings of 2nd International Conference on UHPC Materials and Structures, Fuzhou, 2018.
[41] U. Diederichs, O. Mertsch, Behaviour of Ultra High Strength Concrete at high temperatures, in: E. Fehling, M. Schmidt, S. Stürwald (Eds.), Proceedings of the 2nd International Symposium on Ultra High Performance Concrete, 2008, pp. 347–354.
[42] R. Felicetti, P.G. Gambarova, M.P. Natali Sora, G.A. Khoury, Mechanical behaviour of HPC and UHPC in direct tension at high temperature and after cooling, in: in: Proceedings of BEFIB – 5th Symposium on Fibre-Reinforced Concrete, 2000, pp. 749–758.
[43] R.T. Way, K. Wille, Effect of heat-induced chemical degradation on the residual mechanical properties of ultrahigh performance fibre-reinforced concrete, J. Mater. Civ. Eng. 28 (4) (2016) 04015164, https://doi.org/10.1061/(ASCE)MT.1943-5533.0001402.
[44] Vahid Afroughsabet, Luigi Biolzi, Paulo J.M. Monteiro, The effect of steel and polypropylene fibers on the chloride diffusivity and drying shrinkage of high-strength concrete, Composites Part B: Engineering 139 (2018) 84–96.
[45] J.-C. Mindeguia, P. Pimienta, A. Noumowé, M. Kanema, Temperature, pore pressure and mass variation of concrete subjected to high temperature – experimental and numerical discussion on the spalling risk, Cem. Concr. Res. 40 (2010) 477–487, https://doi.org/10.1016/j.cemconres.2009.10.011.
[46] Dorjan Dauti, Alessandro Tengattini, Stefano Dal Pont, Nikolajs Toropovs, Matthieu Briffaut, Benedikt Weber, Analysis of moisture migration in concrete at high temperature through in-situ neutron tomography, Cement and Concrete Research 111 (2018) 41–55.
[47] Sun Bei, Lin Zhixiang, Investigation on spalling resistance of ultra-high-strength concrete under rapid heating and rapid cooling, Case Studies in Construction Materials 4 (2016) 146–153.
[48] X. Liu, G. Ye, G. De Schutter, Y. Yuan, L. Taerwe, On the mechanism of polypropylene fibres in preventing fire spalling in self-compacting and high-performance cement paste, Cem. Concr. Res. 38 (2008) 487-499. https://doi.org/10.1016/j.cemconres.2007.11.010.
[49] Xiangwei Liang, Chengqing Wu, Yekai Yang, Zhongxian Li, Experimental study on ultra-high performance concrete with high fire resistance under simultaneous effect of elevated temperature and impact loading, Cement and Concrete Composites 98 (2019) 29–38.
[50] Fadzli Mohamed Nazri, Ramadhansyah Putra Jaya, Badorul Hisham Abu Bakar, Raudhah Ahmadi, A. Hasan, A.A. Khan, Md. A. Mannan, C.N. Hipolito, N. Mohamed Sutan, Al-K. Hj. Othman, M.R. Kabit, N. Abdul Wahab, Fire resistance of ultra-high performance fibre reinforced concrete due to heating and cooling, MATEC Web Conf. 87 (2017) 01021, https://doi.org/10.1051/matecconf/20178701021.
[51] H. Huang, R. Wang, X. Gao, Improvement effect of fiber alignment on resistance to elevated temperatures of ultra-high performance concrete. Composites, part B 177 (2019),107454. https://doi.org/10.1016/j.compositesb.2019.107454.
[52] G. F. Peng, J. Yang, Q. Q. Long, X. J. Nin and Q. P. Zeng, Comparison between Ultra-High-Performance Concretes with recycled steel fiber and normal industrial steel fiber, in: E. Ganjian, N. Ghafoori and P. Claisse (Eds.), Proceedings of 4th International Conference on Sustainable Construction Materials and Technologies, Las Vegas, 2016, paper S312.
[53] J.-H. Lee, Y.-S. Sohn, S.-H. Lee, Fire resistance of hybrid fibre-reinforced, ultra-high-strength concrete columns with compressive strength from 120 to 200 MPa, Magazine of Concrete Research 64 (6) (2012) 539–550.
[54] Jian Yang, Baochun Chen, Camillo Nuti, Influence of steel fiber on compressive properties of ultra-high performance fiber-reinforced concrete, Construction and Building Materials 302 (2021) 124104, https://doi.org/10.1016/j.conbuildmat.2021.124104.
[55] Istruzioni per la progettazione, l'esecuzione e il controllo di strutture in calcestruzzo fibrorinforzato. CNR DT 204/2006, Italian Council for Research, 2008 [in Italian]. https://www.cnr.it/it/node/2624.
[56] Testing hardened concrete - Part 3: Compressive strength of test specimens. Comité Européen de Normation, EN 12390-3, 2009.
[57] C. Gallé, Effect of drying on cement-based materials pore structure as identified by mercury intrusion porosimetry, Cement and Concrete Research 31 (10) (2001) 1467–1477.